RSC Advances

REVIEW

View Article Online
View Journal | View Issue

Cite this: *RSC Adv.*, 2015, **5**, 105003

Methods and strategies for the synthesis of diverse nanoparticles and their applications: a comprehensive overview

Chetna Dhand,[a] Neeraj Dwivedi,[b] Xian Jun Loh,[c] Alice Ng Jie Ying,[a] Navin Kumar Verma,[ad] Roger W. Beuerman,*[ae] Rajamani Lakshminarayanan*[ae] and Seeram Ramakrishna*[f]

Received 20th September 2015
Accepted 26th November 2015

DOI: 10.1039/c5ra19388e

www.rsc.org/advances

Ongoing advances in nanotechnology research have established a variety of methods to synthesize nanoparticles (NPs) from a diverse range of materials, including metals, semiconductors, ceramics, metal oxides, polymers, *etc.* Depending upon their origin and synthesis methods, NPs possess unique physicochemical, structural and morphological characteristics, which are important in a wide variety of applications concomitant to electronic, optoelectronic, optical, electrochemical, environment and biomedical fields. This review provides a comprehensive overview on various physical, chemical and bio-assisted methods largely employed to synthesize and fabricate NPs of varying size, surface characteristics, functionalities and physicochemical behavior. The key applications of nanoparticles have also been discussed.

1 Introduction

'There's Plenty of Room at the Bottom' a revolutionary lecture by Richard Feynman in 1959 has provided a new thought process to the scientific community to miniaturize and advance prevailing technologies.[1] Inspired with this vision and substantiated with tremendous research efforts, a new branch of science called nanotechnology originated.[2] Nanotechnology is basically an amalgamation of two words "Nano" and "Technology" that deals with dimensions and tolerances of less than 100 nanometres, especially the engineering of individual atoms and molecules. With a promise to advance and benefit the society

[a]*Anti-Infectives Research Group, Singapore Eye Research Institute, Singapore 169856. E-mail: lakshminarayanan.rajamani@seri.com.sg; Tel: +65-6576-7276*

[b]*Department of Electrical and Computer Engineering, National University of Singapore, Singapore 117582*

[c]*Institute of Materials Research and Engineering, A*STAR (Agency for Science, Technology and Research), 3 Research Link, Singapore 117602*

[d]*Lee Kong Chian School of Medicine, Nanyang Technological University, Research Techno Plaza, 50 Nanyang Drive, Singapore 635753*

[e]*Duke-NUS SRP Neuroscience and Behavioral Disorders, Singapore 169857*

[f]*Center for Nanofibers and Nanotechnology, Department of Mechanical Engineering, National University of Singapore, Singapore 117576. E-mail: seeram@nus.edu.sg; Fax: +65-68725563; Tel: +65-65162216*

Chetna Dhand is working as a postdoctoral research fellow at Singapore Eye Research Institute, Singapore. She has completed her PhD in Chemistry from University of Delhi in collaboration with National Physical Laboratory, New Delhi, India. Her major research interests include nanomaterials for different biomedical applications including antimicrobial wound dressings and contact lenses, targeted drug delivery, tissue engineering and biosensors.

Neeraj Dwivedi obtained his PhD in Physics from the Indian Institute of Technology Delhi, India. Currently, he is working as a Postdoctoral Research Fellow in the Department of Electrical and Computer Engineering, National University of Singapore, Singapore. His research interest includes material science, thin films and coatings, nanomaterials, MEMS, nanobiotechnology.

through its wide range of applications in medicines, energy, environment, information technology, aerospace science *etc.*, nanotechnology has emerged as a cutting-edge science in this modern era.[3–5] Owing to its capability to display improved characteristics at small dimensions, nanomaterial is considered as one of the crucial components of nanotechnology. Enriched with outstanding physical, chemical, biological, optical and electronic properties, nanomaterials helped in improving the existing technologies and also opened new avenues to develop novel scientific/technological fields. Depending upon the desired application, the nanomaterials can be synthesized in diverse shapes and dimensions as described in Table 1.

Due to its small dimension and exceptional surface properties, NPs have shown great potential for diverse applications. In general, NPs are the most fundamental element of nanomaterials and act as bridging link between the atomic/molecular structures and nanomaterials. The NPs demonstrate size and shape dependent properties, which can be tailored over wide range. Dendrimers, liposomes, polymer micelles, quantum dots are the other structural analogues of NPs, used for various applications.[49,50] Depending upon the type of the material, NPs are used for broad spectrum applications including drug delivery,[51,52] biosensors,[53] bioimaging,[54] molecular tagging,[55] food technology,[56] textile manufacturing,[57] antimicrobial coatings,[58] quantum computers,[59] quantum lasers,[60] energy and environment, *etc.* (discussed in Section 2.4).

To enfold such a broad range of applications, one of the most essential aspects is to understand various possible

Dr Xian Jun Loh is a polymer chemist working in the interdisciplinary field of biomaterials. He is currently a Senior Scientist and the Head of Research Planning at the Institute of Materials Research and Engineering (IMRE) and an Assistant Professor at the National University of Singapore (NUS). He is also an adjunct scientist at the Singapore Eye Research Institute. His main research interests are in the design of supramolecular and stimuli-responsive polymers and hydrogels for biomedical and personal care applications. Currently, he is the author and co-author of 84 journal papers, 11 patents, 10 book chapters and 3 books.

Alice Ng Jie Ying obtained her Bachelor (Hons) degree in Science (Biomedical Sciences) with specialisation in Cancer Biology from University of Bradford, UK. She worked as Research Officer at Anti-Infective Research Group, Singapore Eye Research Institute (SERI), Singapore. Her research focuses is on designing nanoparticles for exploring their applications as drug delivery carriers for eye anti-infectives.

Navin K. Verma completed his PhD and postdoctoral training in Clinical Medicine at Trinity College Dublin, Ireland. In 2013, Dr Verma joined Lee Kong Chan School of Medicine, Nanyang Technological University Singapore, where he is currently an Assistant Professor of Immunology and Cell Biology. His research is focused on the understanding of signal transduction processes involved in the migration and effector functions of T-lymphocytes in health and diseases. He is also studying the underlying mechanisms by which mammalian cells and tissues interact with biologically responsive nanoparticles, nanostructures and polymeric matrices for their potential therapeutic or diagnostic medical applications.

Roger Beuerman is currently Senior Scientific Director of the Singapore Eye Research Institute, Professor of Neuroscience and Behavioral Disorders at DUKE-NUS School of Medicine and Adjunct Professor of Ophthalmology, Yong Loo Lin, School of Medicine at the National University of Singapore. Roger and his colleagues have developed two well-known translational programs: one a broad program in infectious disease, including design of new antimicrobials, animal models and biofilms and the other in biomarkers for diseases such as dry eye, and keratoconus that reveal basic biological information about the disease as well as severity. His group has developed new classes of antibiotics effective against resistant forms of Pseudomonas *and the CREs. He has more than 300 peer reviewed publications and has co-authored three texts in ophthalmology.*

synthesis methods to design desired NPs. Selection of the synthesis method to realize required NPs largely depends on the desired size, appropriate surface properties and the type of concerned material such as metals, semiconductors, ceramics, polymers, *etc.* In present article, we understand and review the key synthesis methods for the preparation of various types of NPs. Synthesis methods are broadly divided into three parts *viz.*, physical methods, chemical methods and bio-assisted methods. In addition, attempts have also been made to provide a brief discussion on the key applications of different types of nanoparticles.

2 Methods for the synthesis of nanoparticles

High-throughput NPs with good and controlled quality are desirable for their commercialization in various fields of applications. There are two basic approaches commonly employed to prepare NPs; (1) top-down approach, where synthesis is initialized with the bulk counterpart that leaches out systematically bit-after-bit leading to the generation of fine NPs. Photolithography, electron beam lithography, milling techniques, anodization, ion and plasma etching are some of the commonly used top-down methods for the mass production of NPs; (2) bottom-up approach, which involves the coalescence or assembling of atoms and molecules to generate diverse range of NPs. Examples of bottom-up approach include self-assembly of monomer/polymer molecules, chemical or electrochemical nanostructural precipitation, sol–gel processing, laser pyrolysis, chemical vapour deposition (CVD), plasma or flame spraying synthesis and bio-assisted synthesis.[61] In general, NP synthesis methods can be divided in three groups – (1) physical methods, (2) chemical methods, and (3) bio-assisted methods (Fig. 1).

2.1 Physical methods for the synthesis of nanoparticles

Physical methods apply mechanical pressure, high energy radiations, thermal energy or electrical energy to cause material abrasion, melting, evaporation or condensation to generate NPs. These methods mainly operate on top-down strategy and are advantageous as they are free of solvent contamination and produce uniform monodisperse NPs. At the same time, the abundant waste produced during the synthesis makes physical processes less economical. High energy ball milling, laser ablation, electrospraying, inert gas condensation, physical vapour deposition, laser pyrolysis, flash spray pyrolysis, melt mixing are some of the most commonly used physical methods to generate NPs.

2.1.1 High energy ball milling (HEBM). High energy ball milling, first developed by John Benjamin in 1970 to synthesize oxide dispersion strengthened alloys capable of withstanding high temperature and pressure, is a robust and energy efficient synthesis method to generate NPs with varying shapes and dimensionalities.[62] In HEBM process, the moving balls transfer their kinetic energy to the milled material. This results in the breaking of their chemical bonds and rupturing of the milled materials into smaller particles with newly created surfaces (Fig. 2a). Milling media, milling speed, ball-to-powder weight ratio, type of milling (dry or wet), type of high energy ball mill (vibrator mill, planetary mill, attritor mill, tumbler ball mill, *etc.*), milling atmosphere and duration of milling regulate the amount of energy transfer between the balls and the material during the process, and thus affect the physical and morphological properties of the resultant nanomaterials. The HEBM process sometimes involve very high local temperature (>1000 °C) and pressure (several GPa) conditions and thus also considered as a mechanochemical synthesis process.

R. Lakshminarayanan obtained his PhD from the Department of Chemistry at the National University of Singapore. He was a recipient of the Singapore Millennium Foundation Post-doctoral Fellow and then worked as Research Associate at the University of Southern California. Currently, he is working as a Principal Research Scientist at the Singapore Eye Research Institute. His major interests include antimicrobial peptides design, topical delivery of antimicrobial peptides and protein aggregation diseases.

Seeram Ramakrishna, FREng, *is the Director of Center for Nanofibers & Nanotechnology at National University of Singapore. He authored 6 books and ~650 ISI listed journal papers, which attracted ~46 419 citations and 100 H-index. He is a highly Cited Researcher in Materials Science. He received several awards and recognitions. He is an elected international fellow of Royal Academy of Engineering, UK; National Academy of Engineering, India; Institution of Engineers Singapore; ASEAN Academy of Engineering & Technology; American Association of the Advancement of Science; ASM International; American Society for Mechanical Engineers; Institution of Mechanical Engineers, UK; Institute of Materials, Minerals & Mining, UK; and American Institute for Medical & Biological Engineering. He is an editorial board member of ~10 international journals.*

Table 1 Brief overview on different types of nanostructures, their synthesis methods and related applications

Type of nanomaterials	Synthesis	Applications
Nanocage: First reported in 2002, this class of nanomaterials has hollow interior and porous walls containing metallic nanoparticles (MNPs) inside. Their size ranges between 10–150 nm[6] 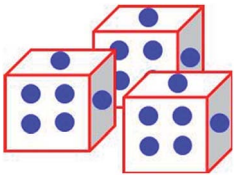	Nanocages can be synthesized by simple template engaged galvanic replacement reaction among the metallic precursor and the nanotemplates of more reactive metals[6,7]	As tracers for tracking using multi-photon luminescence, contrasting agents for photoacoustic and multimodal imaging, photothermal agents for the selective destruction of cancerous tissue and drug delivery vehicles for smart release in response to external stimuli such as NIR radiation or high-intensity focused ultrasound[8]
Nanocrystal: Nanocrystal is single or multi-phase polycrystalline solids with grain size of less than 100 nm[9] 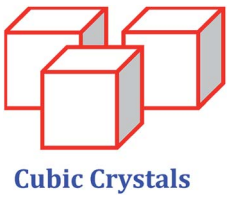	Murray *et al.* have reported high temperature colloidal method to synthesize semiconducting magnetic nanocrystals that are uniform in size to ±one atomic layer, composition, shape, internal structure, and surface chemistry.[10] Li *et al.* have developed an unified liquid–solid–solution phase transfer synthetic strategy to fabricate monodisperse nanocrystals with different chemistries and properties using versatile materials including noble metal, magnetic/dielectric, semiconducting, rare-earth fluorescent, biomedical, organic optoelectronic semiconducting and conducting polymers NPs.[11] Hyeon *et al.* have nicely reviewed the synthesis strategies to design monodisperse nanocrystals of metals, semiconductors and metal oxides[12]	Memory devices, solar cells, solid-state displays, photo-detectors and field-effect transistor (FET) detectors[13,14]
Nanobelt: Nanobelt is thin and flat sheets of ribbon-like structures that are typically 30–300 nm in size.[15] Nanobelts with rectangular cross-section and well-defined crystalline facets enable to attain unique optical confinement, microcavity, catalysis and piezoelectric effect[16] 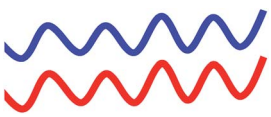	Wang *et al.* have reported the synthesis of 1D ultra-long nanobelts of lanthanum hydroxide using composite-hydroxide-mediated synthesis method[16]	Nanobelts have profound impact in the field of self-powered nanodevices and nanosystems. They have applications in FET devices, nanometer-sized ultrasensitive gas and biosensors, resonators, cantilevers, *etc.*[17]
Nanofiber (NF): These are 2D fibre structures having diameter less than 100 nm 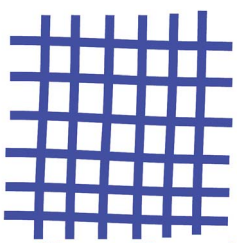	Electrospinning is the most explored method for large scale production of NFs of versatile materials including polymers, metal oxides, carbon based materials, supramolecular dipeptides, *etc.*[18–20] Other method to design NFs are emulsion polymerization, self-assembly, melt blowing and phase separation *etc.*[21–23]	Water filtration systems, surgical implants, biosensors, drug delivery systems, electronic devices, tissue engineering, *etc.*[24–26]
Nanoparticle (NP): According to IUPAC, particle of any shape with dimensions in the 1×10^{-9} and 1×10^{-7} m range is known as nanoparticle (NP) 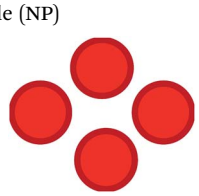	Different chemical, physical and biological strategies are available to design NPs of various material types (polymers, inorganic oxides, metals, *etc.*) of diverse sizes, surface characteristics and topography.[27] Our review is an attempt to compile all the synthesis methods for the NP design	NPs are having a wide range of applications that includes their role in biomedical devices (biosensors, tissue engineering, drug delivery, bioactuators, bio-imaging devices, *etc.*), electronics and optoelectronic devices, food industry, construction industries, *etc.*[28]

Table 1 (*Contd.*)

Type of nanomaterials	Synthesis	Applications
Nanotube (NT) and Nanorod (NR): NT is microscopic tube whose diameter is measured in nanometers (usually <100 nm).[29] NT are mostly hollow. On the contrary NR is solid structure with aspect ratio of ~3–5 and each of their dimension from 1–100 nm[30]  Nanotubes  Nanorods	Arc-discharge, laser ablation, and chemical vapour deposition (CVD) are some of the methods used to prepare metallic/semiconducting nanotubes and nanorods.[31] Emulsion polymerization method is another chemical strategy to design soft nanotubular structures[32]	Nanotubes specifically carbon nanotubes (CNT) has the potential to design wonder technologies. CNT yarns and sheets have already been known to have promising applications in supercapacitors, actuators and electromagnetic shields.[29,33] Continuous efforts are under progress to use these nanostructures in biomedical fields and nanomedicines[34]
Nanowire (NW): Nanowire is smart 1D nanostructural material with dimensions of the order of 10^{-9} meters	Nanowires can be synthesized both by top-down approach or bottom-up approaches. The commonly used techniques for the synthesis of nanowires are chemical, electrochemical, photochemical, electrophoresis, CVD, physical vapour deposition (PVD), plasma assisted chemical vapour deposition (PACVD), *etc.*[35,36]	Since semiconductor nanowires show tremendous electronic and optoelectronic properties, they can be used for fabrication of p–n junctions, transistors, solar cells, sensors, *etc.*[37,38]
Quantum dot (QD): Quantum dots is nanocrystal of semiconducting material, small enough to exhibit quantum mechanical properties and their excitons are confined in all three dimensions. These exhibits strong size dependent optical and electronic properties. QD can contain as few as 100 to 100 000 atoms within the quantum dot volume, with a diameter of 10 to 50 atoms[39]	Three routes to design QD are: (i) organometallic method that consists of three components *viz.*, precursors, organic surfactants and solvents, (ii) aqueous synthesis using short-chain thiols as stabilising agents, (iii) biological method using microorganisms[40,41]	Due to their superb optical and electronic properties, they can be extensively applied to light-emitting diodes, lasers, biomarkers, biosensor devices and biomedical imaging[41–43]
Nanocomposites: It is multiphase material where at least one of the constituent phases has one dimension less than 100 nm.[44] The promise of nanocomposites lies in their multifunctionality, the possibility of realizing unique combinations of properties unachievable with traditional pristine materials[45] 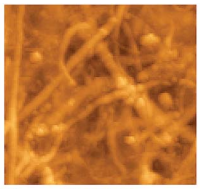 Polyaniline-CNT Nanocomposite	Different chemical, physical and biological methods can be employed to derive different nanocomposites depending upon the materials concerned	Applications of nanocomposites are in microelectronic industry, aerospace, electronic packaging and also in catalysis[46–48]

Using metallic iron powder as the precursor material, Carvalho *et al.* synthesized superparamagnetic magnetite NPs with size ranging from 12 nm to 20 nm by HEBM process.[63] Bartwal and co-workers optimized various milling parameters (milling time, rotation per minute; rpm, ball size, *etc.*) to prepare uniform $LiNbO_3$ NPs with particle size ranging from ~30 to 60 nm.[64] Salah and co-workers synthesized ZnO NPs of ~30 nm size from ZnO microcrystalline powder using HEBM process.[65] Synthesized ZnO NPs showed antibacterial activities due to their desirable lattice constant. Chen *et al.* utilized microwave assisted HEBM method to prepare pure and well-crystallized cobalt ferrite NPs with mean size of 20 nm, and high saturation magnetization (82.9 emu g^{-1}), at low temperature (≤100 °C) without subsequent calcination.[66] Cobalt oxalate hydrate and Fe powder were used as the raw materials for this synthesis and stainless steel or pure iron balls with diameter of 1.5 mm were used for milling. Xing *et al.* recently established HEBM as the powerful green synthesis method for

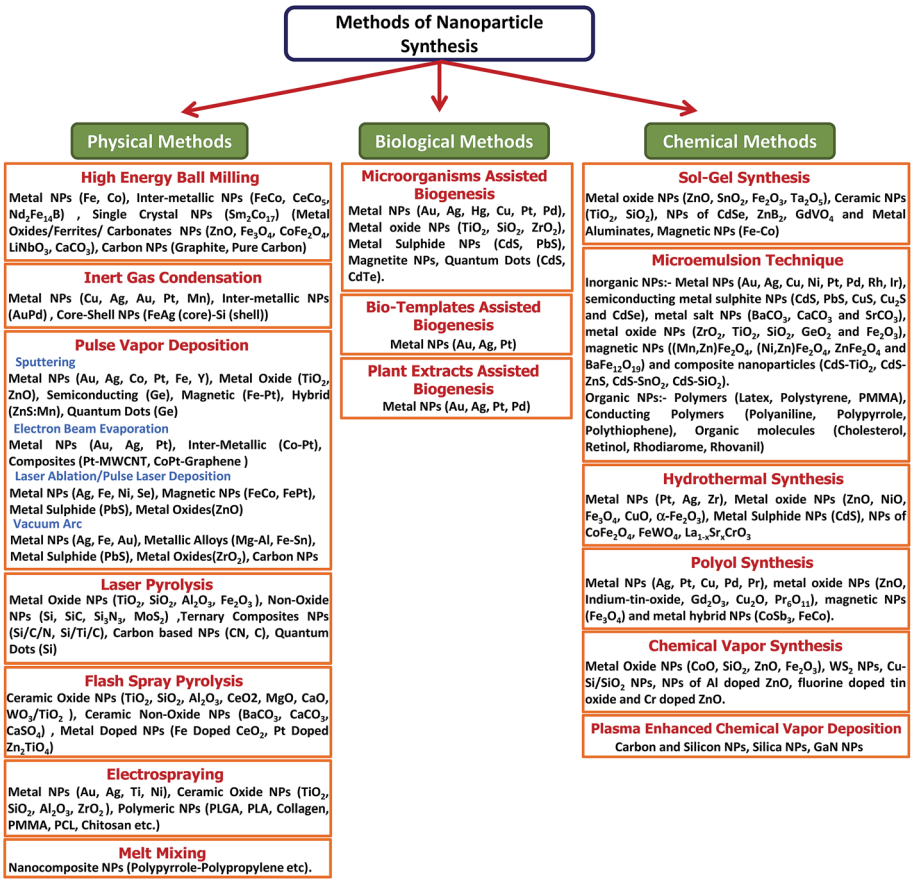

Fig. 1 Overview on different type of synthesis methods to produce variety of nanoparticles.

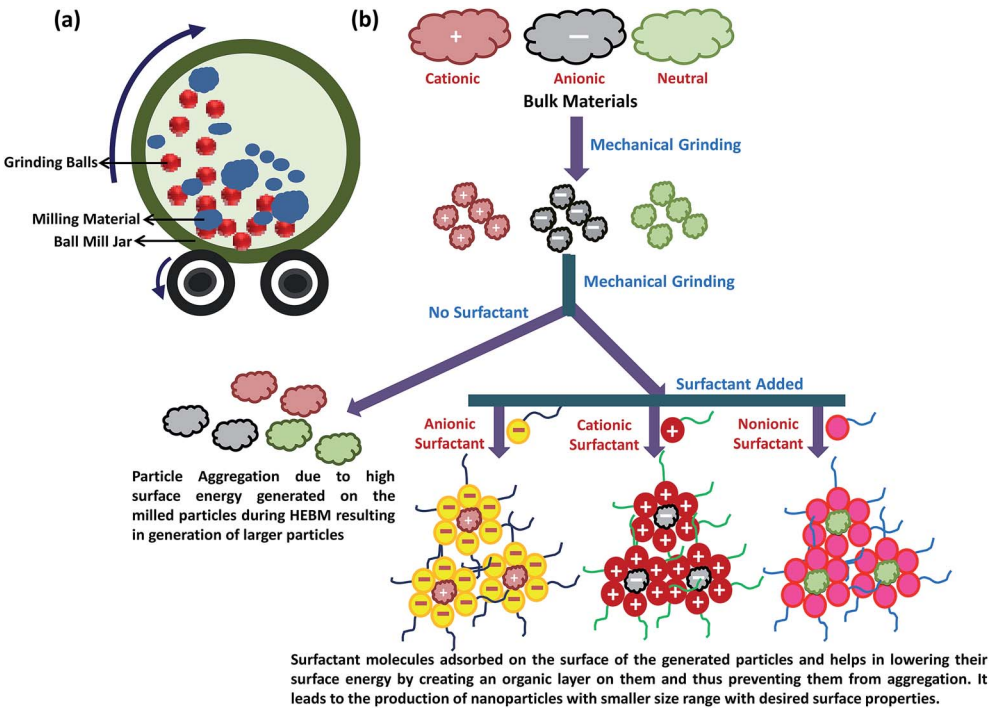

Fig. 2 (a) High energy ball milling (HEBM) system and (b) schematic representation of the NPs synthesis using HEBM method with and without surfactant.

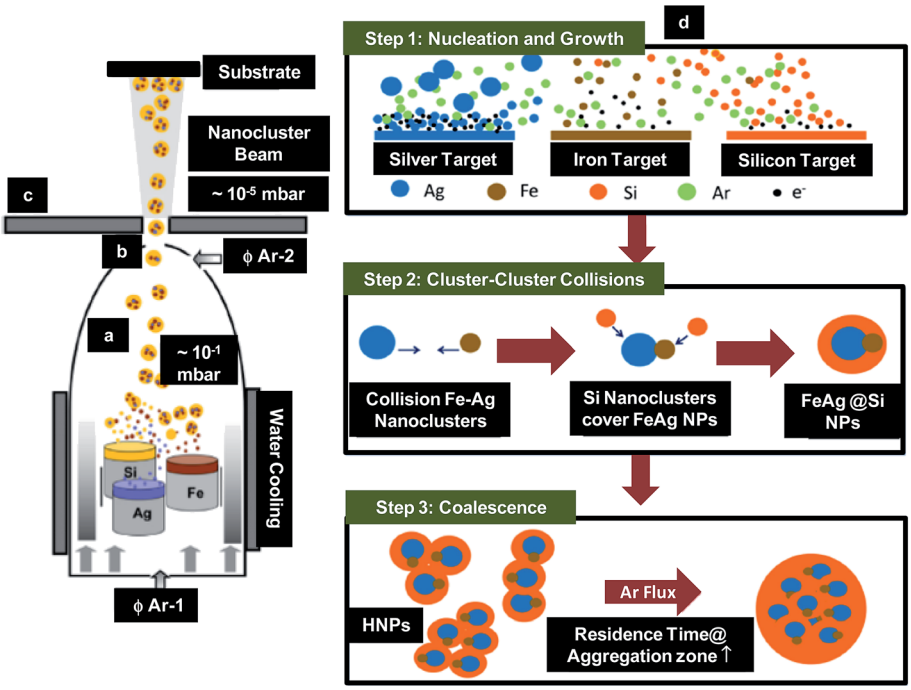

Fig. 3 Schematic showing (a)–(c) IGC system used for synthesis of HNPs; (a) aggregation zone, (b) aperture through which formed nanoclusters moved and (c) deposition section and (d) mechanism responsible for the synthesis of HNPs. Reproduced with permission from ref. 76.

large-scale production of nitrogen doped carbon NPs for catalytic applications.[62]

Currently, surfactant assisted high energy ball milling is used as an efficient strategy for the synthesis of NPs with precise size and specific surface characteristics (Fig. 2b). Surfactants are the surface active agents containing both hydrophobic and hydrophilic properties and can be classified as anionic, cationic, zwitterionic and nonionic depending upon the surface charge characteristics of their hydrophilic group.[67] Following adsorption on the material surface, the surfactant molecules generate electrostatic/steric forces which stabilize the milling particles, and thus minimize the uncontrolled fracturing of particles. Surfactant can also lower the surface energy of the freshly generated fine particles by forming thin organic layer and introducing long range capillary forces that lower the energy for crack propagation. This prevents the particles from agglomeration and cold welding that may lead to enhancement of particle size. Nature and amount of the surfactant used during the HEBM tremendously affect the physical characteristics of the NPs. Normally, increasing the surfactant volume can decrease the particle size by second to third order of magnitude. Zheng *et al.* designed rare-earth-based magnetically hard single-crystal NPs of Sm_2Co_{17} with average diameter of 9 nm and 26 nm by HEBM using oleic acid and oleylamine, respectively, as the surfactant with $SmCo_5$ as precursor.[68] Islam *et al.* used this surfactant assisted HEBM method to prepare pure $CaCO_3$ NPs with diameter of 30 nm from cockle shells using dodecyl dimethyl betaine (BS-12).[69] Surfactant assisted HEBM has also been used to synthesize graphite NPs of the size ranging from 1–30 nm,[70] where the carbon black was used as a precursor and phosphate ester as a surfactant in aqueous media.

2.1.2 Inert gas condensation (IGC). Inert gas condensation is one of the primitive methods for the NP synthesis that employ inert gases (*e.g.* He or Ar) and liquid nitrogen cooled substrate holder for the preparation of NPs. The evaporated materials are transported with inert gases and condensed onto the substrate attached with liquid nitrogen. Ward *et al.* used this method for the synthesis of Mn NPs.[71] Perez-Tijerina *et al.* fabricated AuPd NPs using IGC process and studied the effect of annealing on the structure of the deposited NPs.[72] IGC was found to be highly efficient method for the synthesis of good quality silver and platinum NPs.[73] Sputtered deposition unit was used as the source for the generation of these NPs. Raffi *et al.* also reported the synthesis of Ag NPs by IGC method and found a strong dependence of the evaporation temperature (varied between 1123 K and 1423 K) and inert gas (He) pressure (varied between 0.5 and 100 Torr) on the morphology, crystallinity and size distribution.[74] The mean particle size was found to increase with increasing evaporation temperature and He gas pressure and was in the range from 9 nm to 32 nm. Fabrication of size controlled Cu NPs (1–5 nm) was performed using IGC method combined with glow discharge sputtering as a source of Cu NPs.[75]

Benelmekki *et al.* reported the synthesis of metallic-dielectric multi-core–shell NPs by IGC method.[76] The FeAg NPs were deposited in Si shell (Fig. 3a–c), where Si shell protected the NPs against oxidation and restrained their aggregation. The basic principle for the synthesis of such hybrid nanoparticles (HNPs) was based on the condensation of atomic vapor produced from sputtering of multiple targets (Fe, Ag and Si) simultaneously at high pressure. Argon working pressure was kept at 10 mbar during the deposition. Using DC

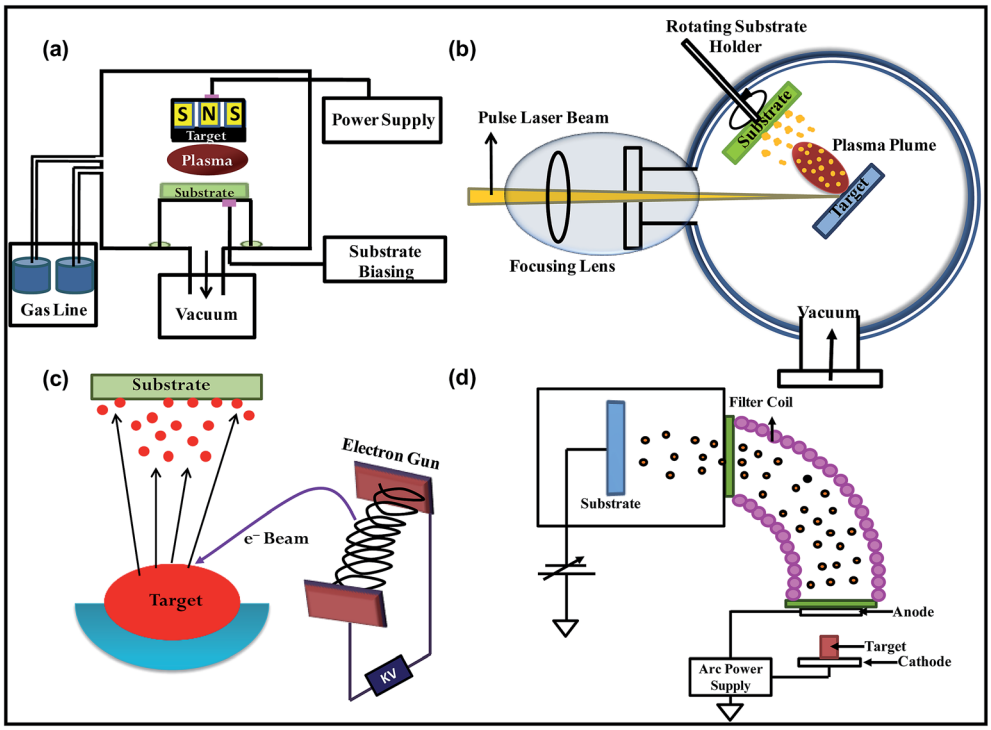

Fig. 4 Schematic representation of (a) plasma sputtering, (b) electron beam evaporation, (c) pulsed laser deposition and (d) vacuum arc technique.

sputtering, vapours of metal atoms were produced near the target surface and condensed into nanoclusters along its propagation path through aggregation zone as shown in Fig. 3a. These nanoclusters were then extracted and accelerated due to difference in pressure between aggregation zone (10 mbar) and deposition unit (10^{-5} mbar) and then deposited onto the substrate (Fig. 3b and c). The mechanism responsible for the fabrication of multi-core–shell HNPs is illustrated in Fig. 3d. The mechanism was divided into three steps. Step 1 was associated with the nucleation and growth of the NPs. Plasma density was found to be an important parameter, which influences the nucleation, growth and crystallinity of the NPs. The plasma density and sputtering yield (~1.2) were maximum in case of Ag. This led to the nucleation and growth of the highly crystalline Ag NPs before leaving the plasma zone, which then quenched into mono-crystalline NPs in aggregation zone. Since the plasma density and sputtering yield (0.45) was lower in case of Fe than Ag, their nucleation and growth occurred when the atoms reached the aggregation zone. This transportation process caused loss of energy of the atoms resulting in the creation of amorphous nanoclusters/NPs. The plasma density and sputtering yield (0.29) was lowest in case of Si leading to the formation of amorphous Si nanoclusters/NPs. Step 2 involve cluster–cluster collisions, where the nanoclusters collide and coalescence with each other in aggregation zone, leading to the formation of larger NPs. However, formation of core/shell or dumbbell-like structures was most probable due to the large positive free energy of Ag and Fe mixing. In other words, during collision in aggregation zone, Ag and Fe nanoclusters could not completely coalescence due to lack of energy. This led to the formation of dumbbell-like structures in amorphous Si matrix. Finally, during their movement through aggregation zone, AgFe/Si core–shell NPs were found to collide and partially coalescence with each other resulting in the formation of multi-core–shell HNPs in step 3. Fabricated HNPs were found to be the promising candidates for magneto-optic bio-applications.

2.1.3 Physical vapor deposition (PVD). Physical vapour deposition is a collective set of processes commonly used to produce NPs and to deposit thin layers of material, typically in the range of few nanometers to several micrometers. PVD is an environment friendly vacuum deposition technique consisting of three fundamental steps: (1) vaporization of the material from a solid source, (2) transportation of the vaporized material, (3) nucleation and growth to generate thin films and NPs.[77] Most commonly used PVD methods for NPs synthesis are

(i) Sputtering
(ii) Electron beam evaporation
(iii) Pulsed laser deposition
(iv) Vacuum arc

Fig. 4 shows the schematics representations of different PVD techniques.

2.1.3.1 Sputtering. Sputtering is a vacuum-based PVD process, which is often used to deposit films and NPs (Fig. 4a). Sputtering works on the principle of momentum transfer in which the atoms from the target (which is made up of material to be deposited) are ejected by the ion bombardment. The deposition of material by sputtering can be achieved using DC,

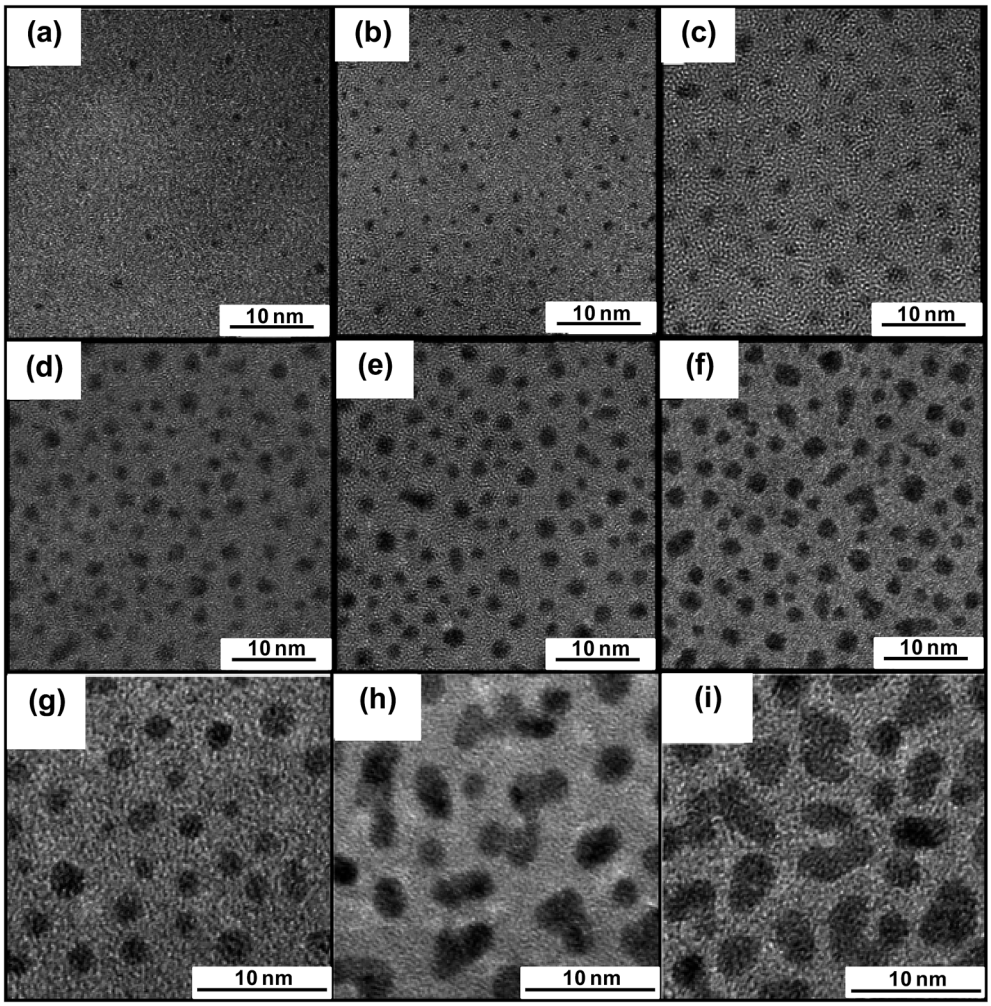

Fig. 5 High resolution transmission electron microscopy images of Pt NPs synthesized by sputtering process. (a)–(f) Pt NPs grown at constant target angle of 23.8° but varied growth time of (a) 5 s, (b) 10 s, (c) 20 s, (d) 30 s, (e) 45 s and (f) 55 s. (g)–(i) Pt NPs grown at constant growth time of 2 min but varied target angle of (g) 16.2°, (h) 23.8° and (i) 38.8°. Reproduced with permission from ref. 85.

pulsed DC and radio frequency (RF) powers. The sputter deposition takes place in following steps:

(i) The plasma of neutral gases, commonly Ar, is generated between the two electrodes by the collisions of electrons to gaseous molecules

(ii) Ions present in the plasma are then accelerated toward the target by applying potential between the two electrodes

(iii) These ions with appropriate energy thus hit the target, leading to ejection of the material from the target

(iv) The ejected material are then transported and deposited onto the substrate

Simple sputtering and magnetron sputtering are two types of sputtering processes. The difference between the two processes arises due to the fact that simple sputtering does not contain magnets behind the target, while magnets are always present in case of magnetron sputtering. The magnetron sputtering is upgraded version of simple sputtering and has following two advantages over former process:

- Higher deposition rate
- Prevent target overheating and damage

Higher deposition rate in magnetron sputtering is obtained due to the fact that under the influence of magnetic field the path of electrons become curved *i.e.* they follow helical path. This leads to more ionization of gases, causing more ions hit to the target, and hence results in higher deposition rate. In sputtering, sputtering yield is an important parameter, which describes the number of atoms ejected per incident ions. It should be noted that DC sputtering can be used to deposit nanostructures of conducting materials, while the deposition of insulating material by DC sputtering is difficult. However, RF sputtering can be used for the deposition of insulating materials also. Further, when reactive gases are introduced into the sputtering process chamber then sputtering process can be called as reactive sputtering. Reactive sputtering is used to deposit variety of compound/hybrid materials.

In all types of sputter deposition processes the NPs of ideal size can be synthesized by selecting the appropriate deposition conditions. For example, Hatakeyama and Nishikawa have synthesized Au NPs by analytically varying the sputtering conditions that influences the particle size and its

Table 2 Various nanoparticles synthesized using PLD technique[a]

Type of nanoparticles	Deposition medium	Deposition parameters	Size of nanoparticles	Laser type	References
Ag NPs	Aqueous SDS solution	LI: 120 mJ per pulse, RR: 10 Hz, PW: 5 ns, TTS distance: 4.5 mm	4.2 ± 1.9 nm in SDS (anionic surfactant)	Nd:YAG laser, 532 nm	94
	Aqueous CTAB solution	LI: 120 mJ per pulse, RR: 10 Hz, PW: 5 ns, TTS distance: 4.5 mm	7.8 ± 4.5 nm in CTAB (cationic surfactant)		
	Aqueous SDS solution	LI: 60 mJ per pulse, RR: 10 Hz, PW: 5 ns, TTS distance: 4.5 mm	6.8 ± 2.7 nm in SDS		
	Aqueous CTAB solution	LI: 60 mJ per pulse, RR: 10 Hz, PW: 5 ns, TTS distance: 4.5 mm	9.4 ± 5.9 nm in CTAB		
Ag NPs	Ar gas, 70 Pa pressure	BP: 2×10^{-4} Pa, LED: 2 J cm^{-2}, LIA: 45°, TTS distance: 35 mm, NLS: 15 000 & 30 000, RR: 10 Hz	1.5–4.5 nm	248 nm KrF laser	99
Ni NPs	Vacuum	RP: 10^{-5} Pa, LI: 1 mJ per pulse, LIA: 45°, TTS distance: 30 mm, NLS: 200, LED: 0.3 J cm^{-2}	5–100 nm, MS ≈ 40 nm	1 kHz Ti:sapphire oscillator–amplifier system emitting at 780 nm	104
Ni NPs Fe NPs	High vacuum	BP: 5×10^{-7} Torr, RR: 10 Hz, PW: 10 ns, LED: 2 J cm^{-2}, ST: 500 °C	~10 nm 4.5–9 nm	—	101
Se NPs	High vacuum	BP: 8×10^{-4} Torr, PD: 108 W cm^{-2}, PW: 10 ns, LIA: 45°, TTS distance: 35 mm	75–100 nm	Nd:YAG laser, 532 nm	102
ZnO NPs	Aqueous SDS solution	RR: 10 Hz, LI: 100 mJ per pulse, IT: 60 min	9.4–32.1 nm, AD: 14.7 nm	Nd:YAG laser, 532 nm	96
PbS	O_2 gas, 300 mTorr pressure	RR 10 Hz, PW: 30 ns, TTS distance ~ 50 mm, LI: 183 mJ per pulse	10–50 nm, AD: 17 nm	248 nm KrF laser	105
FeCo NPs	Ar gas, pressure varying from 10–90 kPa	BP: 10^{-4} Pa, RR: 10 Hz, PW: 10 ns, ST: 150 °C	4.8–8.6 nm	Nd:YAG laser, 532 nm	98
FePt NPs	Ar gas	BP: 5×10^{-5} mbar, LI: 75 mJ per pulse, LED: 955 J cm^{-2}, TTS distance: 6 mm	4.8–22 nm	Nd:YAG laser, 532 nm	103

[a] Abbreviations: AD – average diameter, BP – basic pressure, CTAB – cetyltrimethylammonium bromide, IT – incubation time, LED – laser energy density, LI – laser intensity, LIA – laser incident angle, MS – mean size, NLS – number of laser shots, PW – pulse width, RP – residual pressure, RR – repetition time, SDS – dodecylsulfuric acid sodium salt, ST – substrate temperature, TTS distance – target-substrate distance.

distributions.[78] Veith *et al.* used magnetron sputtering for the deposition of Au NPs on WO_3 and activated carbon surfaces.[79] Using magnetron sputtering and selecting the appropriate deposition parameters, Bouchat *et al.* reported the synthesis of variety of metallic and non-metallic NPs including titanium oxide (TiO_2), silver (Ag), gold (Au), yttrium (Y), carbon (C), cobalt (Co) and iron (Fe).[80] Asanithi *et al.* optimized the process conditions for the deposition of uniform sized, <10 nm, silver NPs by DC magnetron sputtering.[81] While varying target-to-substrate (TTS) distance from 10 to 20 cm, they demonstrated significant tailoring of particle size with the formation of highly uniform small grains (3.8 ± 0.7 nm) at optimized TTS distance of 20 cm. Moreover, TTS was also reported to influence the shape and distribution of the Ag NPs. They further tuned the sputtering current (50 mA) at optimized TTS to design monodisperse Ag NPs. However, at higher sputtering current worm-like morphology with increased grain size was obtained. Ichida *et al.* synthesized germanium (Ge) NPs and Ge quantum dots (Ge QDs), both used in electronic and optoelectronic industry, by high pressure RF magnetron sputtering.[82]

Ghosh *et al.* fabricated Mn doped ZnS NPs (ZnS:Mn) by RF magnetron sputtering and studied their photoluminescence and field emission properties.[83] At an optimum Mn concentration, the excellent photoluminescence and field emission properties in ZnS:Mn NPs were realized. In another work, Veith *et al.* fabricated 2 nm size Au NPs on γ-Al_2O_3 using one step magnetron sputtering process which was comparable to those obtained by traditional chemical methods.[84] Ramalingam *et al.* employed tilted-target sputtering in order to grow sub-2 nm sizes and density tuneable Pt NPs at room temperature.[85] They showed that tilting of target angle and variation of growth time significantly altered the mean diameter and density of Pt NPs (Fig. 5).

Sputtering process is also widely used for the synthesis of magnetic NPs for numerous applications. For example, Zhang *et al.* demonstrated the synthesis of $L1_0$ ordered FePt NPs on MgO substrate by DC magnetron sputtering.[86] The FePt NPs were grown at base pressure of 5×10^{-7} Torr and low argon pressure of 1.5×10^{-3} Torr at 750 °C. During the deposition of FePt NPs the sputtering rate was 1.2 Å s^{-1}. Takahashi *et al.* synthesized FePt NPs by sputtering method and studied the effect of size on ordering of the NPs.[87] They suggested that there is a critical value of size of NPs for ordering *i.e.* FCC FePt NPs with size <4 nm diameters do not display $L1_0$ ordering. Further, Dmitrieva *et al.* fabricated FePt NPs by sputtering process and suggested that inclusion of nitrogen during NP deposition can enhance the $L1_0$ phase of FePt NPs.[88]

2.1.3.2 Electron beam evaporation (EBE). Electron beam evaporation is a vacuum-based PVD process which is used to

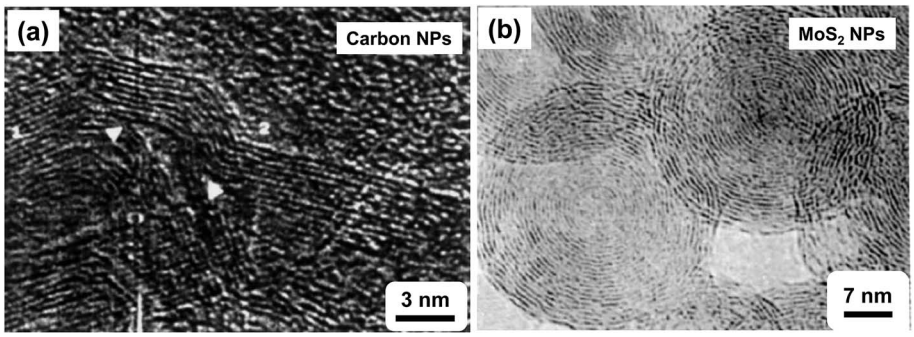

Fig. 6 (a) High resolution electron microscopic image of thin film of carbon cross-linked NPs and (b) high resolution transmission electron microscopic image of thin film of fullerene-like MoS_2 NPs. Reproduced with permission from ref. 108 and 109.

fabricate thin films and NPs. EBE system consists of vacuum unit, electron beam source and target materials (Fig. 4b). Electron beam source consists of a filament, which is heated by passing current through it resulting in the generation of electron beam. The generated electron beam is focused and then directed onto the target material using magnets. The deposition of films by EBE takes place in the following steps:

(i) Electron beam hits the target and heat the target material

(ii) Target material (atoms) evaporates when temperature reaches above its boiling point

(iii) Evaporated material then transported and

(iv) Condensed onto the substrate

Advantage of EBE methods are

(i) High deposition rate

(ii) Can be used to deposit materials ranging from conducting to insulating

(iii) Unlike thermal evaporation, EBE can be used to deposit materials of higher boiling point

By selecting optimum process parameters and conditions during EBE process, NPs of different sizes and shapes can be deposited. Perry *et al.* have reported the use of EBE in the development of NPs for both 2D and 3D metal patterning.[89] Hsieh *et al.* synthesized Au NPs and Pt NPs on multiwall carbon nanotubes (MWCNTs) to form composite electrodes for sensors and energy storage applications.[90] They observed that the distribution of Au NPs was better on MWCNTs than Pt NPs. Uhm *et al.* demonstrated the fabrication of antibacterial Ag NPs on diameter-controlled TiO_2 nanotubes by facile EBE process.[91] Further, Castaldi *et al.* prepared CoPt NPs of size between 5 nm and 20 nm on thermally oxidized silicon using EBE process and found that the size of NPs was dependent on the thickness of the CoPt layer.[92]

Using EBE process, Bello *et al.* fabricated Ag NPs decorated three dimensional graphene (GR) scaffold for electrochemical application.[93] In comparison to pure GR electrode, the GR/Ag NPs electrode showed higher capacitive performance and better cyclability for supercapacitor applications.

2.1.3.3 Laser ablation (LA) and pulse laser deposition (PLD). Laser ablation method utilizes a high power laser beam that evaporates particles from a solid source.[94] In normal LA process, the laser can be either continuous laser or pulsed laser. LA offers a flexible approach in the production of micro- and nano-structures of polymeric materials. Kris *et al.* reported a micro-lens assembly with the utilization of LA technique by scanning the polymer surface to achieve a lens shape with the optimal focal distance and diameter.[95] Gopal *et al.* have synthesized colloidal zinc metallic NPs using the LA technique.[96]

PLD is another vacuum-based PVD process that employs laser energy to remove the material from the target. The high power laser pulses hit the surfaces of target, leading to melting, evaporation and ionization of the material (Fig. 4c). Finally the ablated materials deposit onto the substrate. PLD utilize pulsed laser beam, mainly coming from either excimer laser or Nd:YAG laser, for the ablation of the material. PLD is used for the preparation of variety of materials including polymers, oxides, metallic systems, fullerenes, carbides, nitrides, *etc.*

In context to NPs production, Lee *et al.* reported the synthesis of FeCo NPs in an inert gas atmosphere by PLD.[97] Ong *et al.* examined the role of process parameters such as number of pulses, ambient gas pressure and temperature gradient on the morphology and size of FeCo NPs synthesized by PLD.[98] The morphology of FeCo was changed from linear interconnected chains to fibrous when the number of pulses were increased. At low pressure, NPs tend to form floccules-like nano-networks while chain-like network was observed at higher pressure.[98] In addition, the average size of NPs was increased with increasing gas pressure. Andrea *et al.* used PLD for the synthesis Ag NPs arrays for surface enhanced Raman scattering (SERS).[99] They controlled the size and morphology of Ag NPs by optimizing the Ar pressure and number of pulses. In another work, Jing *et al.* deposited Ag NPs on nickel hydroxide nanosheet arrays using PLD for application to SERS.[100] They found that deposition time influenced the size and inter-particle gap of Ag NPs and hence could control the SERS enhancement. Kumar *et al.* synthesized self-assembled magnetic NPs by PLD and demonstrated the embedment of Fe NPs and Ni NPs of sizes 5–10 nm in amorphous alumina and crystalline TiN materials.[101] Quintana *et al.* performed an interesting work involving the fabrication of selenium (Se) NPs on three different substrates: (1) metallic Au film, (2) Si wafers and (3) glass using PLD.[102] While analyzing the morphology of the deposited NPs, they found that size, shape and population density of Se NPs were strongly dependent on the experimental process parameters and underlying base such as energy density, number of pulses and substrate.

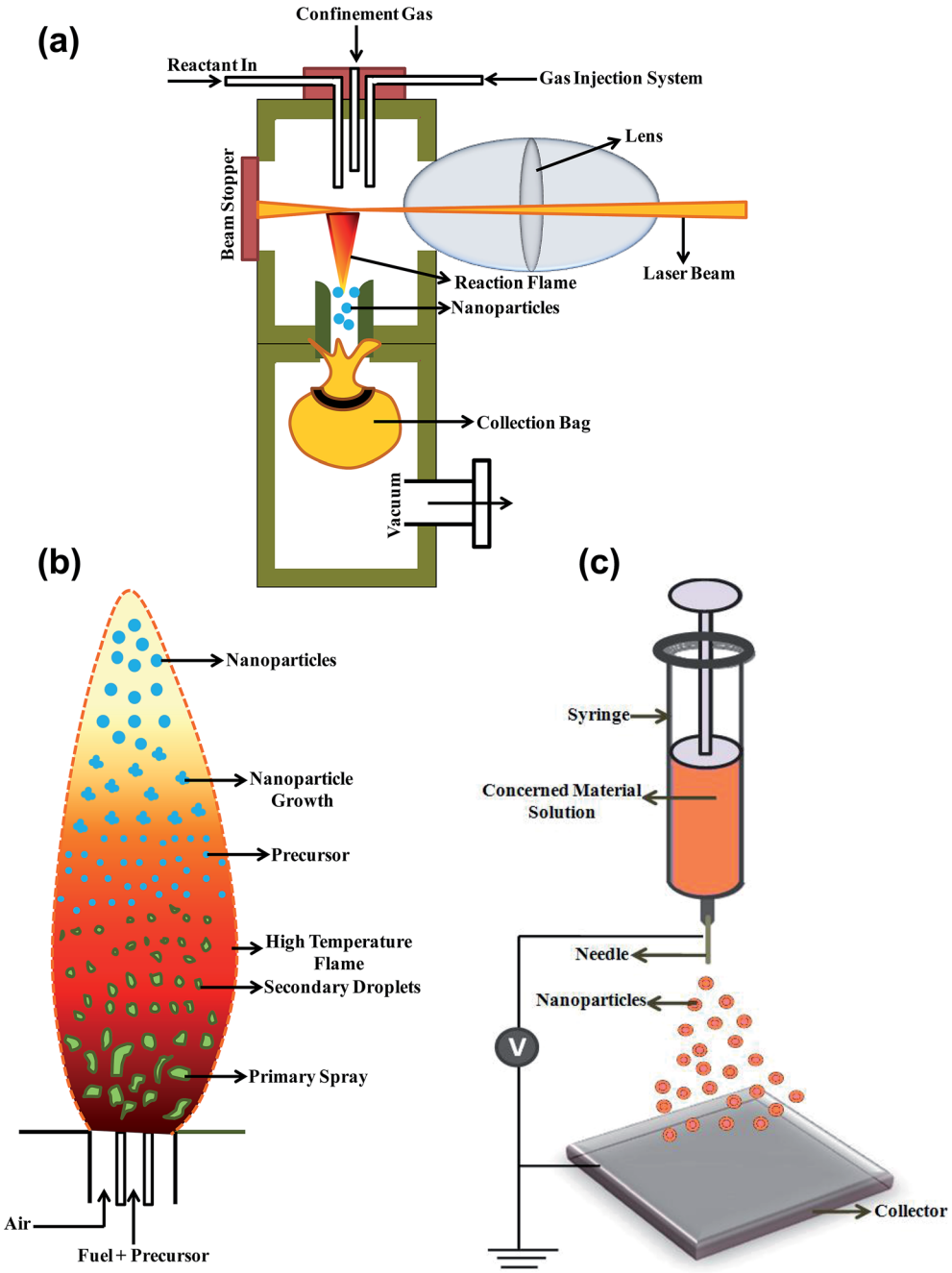

Fig. 7 Schematic illustration of (a) laser pyrolysis, (b) flame spray pyrolysis and (c) electrospraying technique for the synthesis of NPs.

Lin *et al.* studied the effect of target–substrate geometry and ambient gas pressure on the synthesis of FePt NPs by PLD.[103] They suggested that backward plume, which is a novel target–substrate geometry can produce FePt NPs with high uniformity, better phase formation than conventional PLD process. Amoruso *et al.* fabricated Ni NPs by femtosecond PLD, which was confirmed by atomic force microscopy (AFM).[104] Dhlamini *et al.* reported the synthesis of lead sulphide (PbS) NPs in amorphous SiO_2 matrix on Si substrate using PLD and realized excellent photoluminescence properties.[105] Table 2 covers different NPs synthesized by the PLD method with the process details.

2.1.3.4 Vacuum arc (VA). Vacuum arc is a vacuum-based PVD process in which the arc is used to vaporize the material for the synthesis of metallic, ceramic and composite NPs and films (Fig. 4d). Akbari *et al.* synthesized the Mg–Al alloy NPs by varying Mg and Al concentrations using plasma arc process.[106] Lei *et al.* used vacuum arc discharge process for the synthesis of inter-metallic Fe–Sn NPs.[107] Amaratunga demonstrated the synthesis of thin film of linked carbon NPs using localized high pressure arc discharge process and realized excellent mechanical properties in deposited material.[108] Chhowalla and Amaratunga used a similar approach of localized high pressure arc

discharge for the synthesis of thin film of fullerene-like MoS_2 NPs, which showed extremely low friction.[109] Fig. 6a and b show the high resolution electron microscope images of thin films of cross-linked carbon NPs and fullerene-like MoS_2 NPs, respectively.

2.1.4 Laser pyrolysis. The CO_2 laser pyrolysis technique is a vapour phase synthesis process.[61,110] This method can be used to synthesize NPs of large variety of oxide (TiO_2, SiO_2, Al_2O_3, Fe_2O_3), non-oxide (Si, SiC, Si_3N_3, MoS_2) and ternary composites like Si/C/N and Si/Ti/C. In this process, the resultant condensable products are generated from the laser-induced chemical reactions at the interface of the laser beam and the molecular flow of gaseous/vapour phase reactants (Fig. 7a). One of the criteria to induce energy coupling into the reaction system is that one of the reactant/precursor should be able to absorb through resonant vibrational mode of infra-red (IR) CO_2 laser radiations. Alternatively, additional chemicals like ammonia (NH_3), sulphur hexafluoride (SF_6), ethylene gas (C_2H_4), *etc.* are introduced among the reactants as inert photo-sensitizers to accomplish the energy transfer process between the laser light and precursors. The high power of the CO_2 laser initiates the sequential absorption of several IR photons in the same molecule, followed by collision assisted energy pooling, leading to a rapid increase of the average temperature in the gas through vibration-translation energy transfer processes, often accompanied by the appearance of a flame in the interaction volume. If molecules are excited above the dissociation threshold, molecular decomposition, eventually followed by chemical reactions, occurs with the formation of condensable and/or volatile products. Compared to other vapour phase methods, the laser pyrolysis permits highly localized and faster heating (leads to rapid nucleation) with faster quenching of the particle growth (in few ms). Thus, this methodology is promising in generating NPs of the average diameter ranging between 5 to 60 nm with a narrow size distribution in the hot zone. However, as soon as the NPs escape the hot chamber, they try to aggregate resulting in the formation of NPs chains. High energy ball milling and high-power ultrasonic treatment are the effective mechanical processes that help in generation of well-separated NPs using laser pyrolysis method.

Rosaria D'Amato *et al.* utilized laser pyrolysis technique to synthesize variety of ceramic NPs (*e.g.* SiC, SiO_2 and TiO_2) for energy applications and cultural heritage preservation using silane (SiH_4), tetraethyl orthosilicate ($Si(OC_2H_5)_4$) and titanium(IV) isopropoxide respectively as precursor materials.[110] Owing to the advantage of single step doping in this method, Scarisoreanu *et al.* synthesized carbon coated TiO_2 NPs for photocatalysis applications.[111] Marino *et al.* synthesized carbon nitride NPs with varying nitrogen incorporation between 2% and 20% using laser pyrolysis.[112] Jansa *et al.* fabricated carbon NPs using pulsed laser pyrolysis of hydrocarbons and found that at same experimental parameters, the carbon NPs produced using benzene showed higher conductivity than those produced using either acetylene or ethylene.[113] They also found the variation of size of NPs with varying laser power.

Silicon carbide (SiC), silicon and molybdenum disulphide (MoS_2) NPs have also been produced by the laser pyrolysis technique using the same technique.[114] Veintemillas-Verdaguer *et al.* synthesized magnetic composites Fe-based NPs encapsulated in carbon/silica (C/SiO_2@Fe) or carbon (C@Fe) with average diameter of 29 ± 3 nm and 56 ± 3 nm, rerspectively.[115] Laser pyrolysis of the carbonyl precursors is emerging as an excellent technique for the direct synthesis of iron NPs with smaller particle size, narrow size distribution without much noticeable aggregation. Following the same lines, Bomat *et al.* have prepared the iron–iron oxide core–shell NPs (10–30 nm) by laser pyrolysis of $Fe(CO)_5$ vapours and *in situ* passivation by controlled oxidation process.[116] Erogbogbo *et al.* have reported the synthesis of biocompatible Si QD by laser-driven pyrolysis of silane using phospholipid micelles for the imaging of cancer cells.[117]

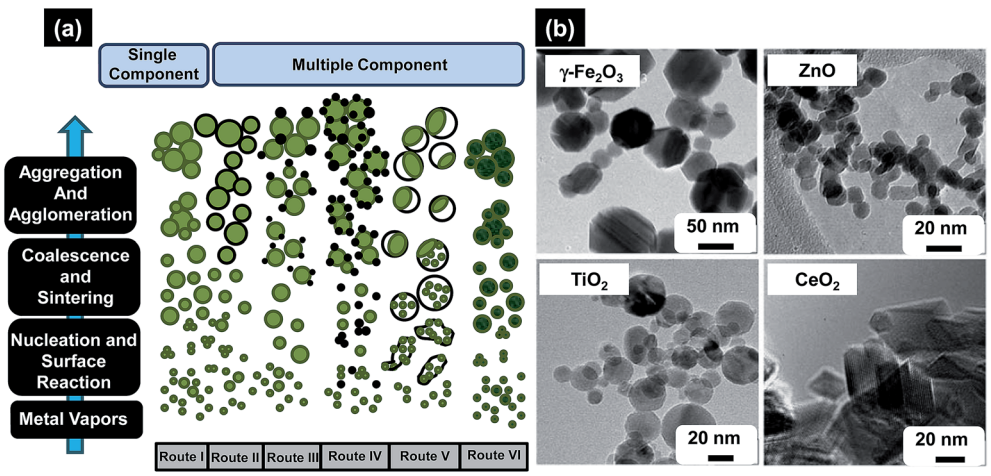

Fig. 8 (a) Formation of different particle configurations *via* the gas-to-particle mechanism for single and multicomponent systems, (b) as-prepared metal oxides NPs of different morphologies made by FSP, varying from hexagonal/octagonal platelet g-Fe_2O_3, lightly oblongated ZnO, spherical TiO_2, and rhomboid-shaped CeO_2 with sharp edges. Reproduced with permission from ref. 118.

Table 3 Different types of NPs synthesized using electrospraying method and their field of applications[a]

Type of nanoparticles	Solvent	Size	Application	References
Au NPs	Water + methanol	20–100 nm	Biomedical field, cancer nanotechnology, molecular imaging, molecular diagnosis, targeted therapy and bioinformatics	133 and 134
Ag NPs	Toluene	3–7 nm	Biosensor, anti-reflection coatings, artificial joint replacement, cancer diagnosis, anti-bacterial activity	135 and 136
Sn NPs	Isopropyl alcohol	3 nm	Humidity sensor, microelectronics and batteries	137 and 138
SiO_2 NPs	Ethylene glycol	20 nm	Photodynamic therapy, magnetic resonance imaging, optical imaging, drug delivery, gene delivery and protein delivery	139 and 140
Si NPs	1-Octanol	3 nm	Biological interface devices, anti-cancer drug delivery and cancer detection	139 and 141
Al_2O_3 NPs	Ethanol	500 nm	Catalysis, waste water treatment, heat transfer fluidics, biosensors, drug delivery and nanocomposites	139 and 142
Ni NPs	Ethylene glycol monoethyl ether acetate + alkylnaphthalene + polyamine	2–3 nm	Magnetism, energy technology and biomedicine	139 and 143
TiO_2 NPs	1-Butanol	10–40 nm	Drug delivery, cosmetics, anti-bacterial materials, sun-screens and electronics	139 and 144
ZrO_2 NPs	1-Butanol	10–40 nm	Catalysis, anti-corrosion coating in surgical appliances, explosive primers, dental implant material, cell and tissue engineering	139,145 and 146
Pt NPs	Ethanol	8 nm	Chemotherapy, cellular imaging, MRI, sun-screen protection and anti-septic products	147 and 148
PLGA NPs	Acetonitrile and dimethyl sulfoxide	165 nm to 1.2 μm	Nanocarriers for drug delivery, cancer diagnosis and imaging	131 and 149
PLA NPs	Butanol/methylene chloride mixture	100 nm	Drug encapsulation, thin film deposition and biomedical engineering	150 and 151
PMSQ NPs	Ethanol	62 ± 20 nm	Organic thin film insulator and printed electronics	152 and 153
PMMA NPs	Acetone	300 nm	Drug/SiRNA systems, artificial enzymes and photostable bio-imaging agents	154 and 155
PCL NPs	Chloroform	4.8 ± 0.2–17.7 ± 0.5 μm	Pharmaceutics, drug delivery, cancer treatment and cell culture	156–158
COLL/NaCl NPs, COLL/$CaCl_2$ NPs	Acetic acid	900 nm (COLL/NaCl) or 630 nm (COLL/$CaCl_2$)	Biomedical and therapeutics, nanomedicine	159 and 160
Chitosan NPs	Acetic acid	520 nm	Anti-cancer treatment, drug delivery, gene delivery and growth factor carriers	161 and 162

[a] Abbreviations: PLGA – poly(lactic-*co*-glycolic acid), PLA – poly-DL-lactic-acid, PMSQ – polymethylsilsesquioxane, PMMA – poly(methyl methacrylate), PCL – polycaprolactone, COLL – collagen.

2.1.5 Flame spray pyrolysis (FSP). FSP is the latest of all the flame aerosol technologies.[118] It is a one-step combustion process where the precursor is in liquid form, with significantly higher combustion enthalpy (>50% of total energy of combustion), usually in an organic solvent. The important technological elements of this process include self-sustaining flame, usage of liquid feeds and less volatile precursors, proven scalability, high temperature flames and large temperature gradients (Fig. 7b). It is one of the most exploited techniques for the production of complex and functional NPs. For the formation of particles, the liquid precursor can follow the droplet-to-particle route or gas-to-particle route; however, later results in more homogenous morphologies and size. For NPs fabrication, precursor spray has to follow the sequential steps *viz.*, (1) precursors evaporate/decompose forming metal vapors; (2) nucleation as a result of supersaturation; (3) growth by coalescence and sintering; and (4) particle aggregation (by chemical bonds) and agglomeration (by physical interactions) (Fig. 7b). Fig. 8 summarise all the particle configurations (and combinations) obtained by FSP. FSP of single metal component precursors in open ambient (air) condition produces simple oxides or carbonates in the case of alkaline metals through reaction with the CO^{2-} laden flame and follow Route I (Fig. 8) for the NPs synthesis. NPs of wide range of elements across the periodic table, from MgO to Yb_2O_3, have been synthesized *via* this route. FSP of metallic NPs including Co, Bi and Cu (following Route II in Fig. 8) have been reported under the anaerobic conditions that helps preventing rapid oxidation of Bi to Bi_2O_3 and resulting in the formation of the protective surface oxide or carbon layer on the Co and Cu NPs. For the multicomponent systems, the particle formation pathways are much more complicated and follow different routes (Route III–VI, Fig. 8).

Sokolowski *et al.* first utilized this strategy to synthesize Al_2O_3 NPs by combusting an ultrasonically-dispersed spray of aluminium acetylacetonate in benzene–ethanol solvent mixture.[119] Later, FSP process was used tremendously to design various oxide and non-oxide ceramic NPs *e.g.* CeO_2, SiO_2, Al_2O_3, MgO, C–Cu, $BaCO_3$, CaO, $CaCO_3$, $CaSO_4$, *etc.* Madler *et al.* adequately reviewed the research articles concerning the design and fabrication of NPs by FSP method and also tabulated very nicely all different oxide and non-oxide ceramic NPs synthesized using this method.[118] Some of the most notable applications of the FSP derived NPs are in the areas of catalysis optics and photonics, sensors, health care, magnetic materials, *etc.*[120–123] For example, Arutanti *et al.* fabricated WO_3/TiO_2 NPs by flame-assisted spray pyrolysis and explored them for photocatalysis.[124] They studied the role of amount of WO_3 and TiO_2 in the range 0–100 wt% on size, shape, crystallinity, and photocatalytic performance. While analyzing the results they found that photocatalytic performance of composite WO_3/TiO_2 NPs was superior compared to 100 wt% TiO_2 catalyst. Channei *et al.* synthesized Fe-doped CeO_2 NPs with varying amount of Fe using flame-assisted spray pyrolysis for photocatalysis application and found that photocatalytic efficiency was 100% when 2 mol% Fe was introduced in CeO_2.[125] Similarly Siriwong *et al.* synthesized Pt-doped Zn_2TiO_4 NPs with varying amount of Pt from 0.25–1.0 mol% using flame-assisted spray pyrolysis and suggested promising use of this process for the synthesis of high quality and controlled sized NPs.[126]

2.1.6 Electrospraying technique. Electrospraying is a technique similar to electrospinning that differs in the type of materials to be produced. The former is done to synthesize NPs while the latter is done for the fabrication of nanofibers.[127] The electrospraying method is based on an electromechanical device in which a mixture of solution containing the selected polymer and the solvent is taken up by the syringe, and a high voltage is applied to the capillary tip that results in the production of charged droplets (Fig. 7c). The solvent is evaporated on its way to the counter electrode and particles or fibers are then collected as the end product. The electrospraying technique provides both flexibility and control of the surface parameters.[128] Deppert *et al.* have reported distinct NPs deposition and the formation of gold NPs for nanostructure growth by utilizing the electro-spraying technique.[129] Sridhar *et al.* reported a comprehensive review over the use of electrospraying technique to produce lipid-based delivery systems and biodegradable polymer NPs as carriers for drug delivery in application to a wide variety of therapeutic area such as cancer therapy, anti-inflammatory, antibacterial agents, *etc.*[130] Maedeh *et al.* reported the assembly of core–shell PLGA NPs encapsulating the protein, bovine serum albumin, by 'coaxial' electrospraying method that can be applied in the management of various severe diseases.[131] Advantages of utilizing electrospraying technique include the ability to generate uniform NP size, fast preparation method and the capability for bulk assembly of NPs. However, this method can also lead to degradation of some macromolecule as a result of thermal or shear stresses in drying and in the syringe.[130]

The electrospraying technique can also be utilized to transform water vapour present in the atmosphere into engineered water nano-structures (EWNS). The EWNS has a size of 25 nm that is equipped with an extraordinary set of physical, chemical, biological and morphological properties with low toxicity level that possess a remarkable mechanism of action as EWNS is loaded with reactive oxygen species (ROS) that is able to interact with and to stop the activity of harmful airborne bacteria.[132] With the electrospraying method, NPs of various type and sizes can be synthesized based on the use of a variety of solvents (Table 3).

2.1.7 Melt mixing. This method involves the mechanical mixing of a polymer with modified nanofillers by extrusion or kneading, and less commonly by injection moulding technique.[163] This is one of the oldest methods to design polymer composites with NPs as the fillers to achieve desired material characteristics. This is the most commonly used mechanical process because it is environment friendly and it is also well-suited for current industrial practices.[164]

Zuhal *et al.* have utilized the melt mixing technique to prepare nanocomposite NPs of conducting polymer polypyrrole with polypropylene and the resultant NPs have been then processed further using injection moulding technique.[165] Weiss *et al.* have reported *in situ* formation of hybrid NPs during melt

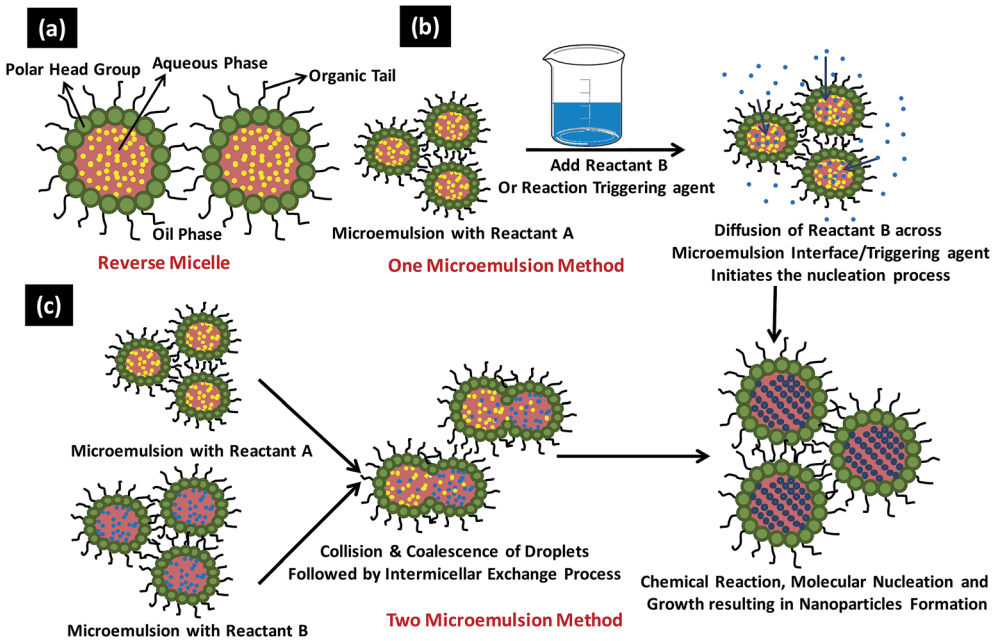

Fig. 9 Shows (a) typical reverse micelle system, (b) various steps involved in one microemulsion process and (c) reaction sequence involved in the two microemulsion nanoparticles synthesis.

blending of hydroxybenzoate (HBA) and 27% hydroxynaphthanoate liquid polymer polyesters with zinc salts of sulfonated polystyrene ionomers at elevated temperatures due to chemical reaction that involved the liquid crystalline polyester and residual zinc acetate from the neutralization of the ionomer.[166]

2.2 Chemical methods for the synthesis of nanoparticles

Sol–gel method, microemulsion technique, hydrothermal synthesis, polyol synthesis, chemical vapour synthesis and plasma enhanced chemical vapour deposition technique are some of the most commonly used chemical methods for the NPs synthesis.

2.2.1 Sol–gel method. In the sol–gel processing method, there are two types of components *viz.*, 'sol' which is a colloidal suspension of solid particles in a liquid and 'gel' which are polymers containing liquid. Thus, this process includes the creation of 'sols' in the liquid that lead to the formation of a network of discrete particles or network polymers by the connection of sol particles.[167] Hydrolysis and condensation are the typical steps of sol–gel process, in which the former uses water to disintegrate the bonds of the precursor that is also the first step in formation of the gel phase. This process is then followed by condensation that leads to the formation of nanomaterials after which excess water is removed to determine the final structure of the material. For instance, ZnO NPs were synthesized by this method using zinc acetate dehydrate and triethanolamine (TEA) as the precursors. Since experimental conditions are very important for the synthesis of NPs by sol–gel method, Behnajady *et al.* optimized the synthesis parameters such as precursors, solvent percentage, water percentage, reflux temperature, reflux time, calcination temperature, sol drying method for the fabrication of TiO_2 NPs by this method.[168] High photocatalytic activity from TiO_2 NPs was observed when they synthesized considering isopropoxide as a precursor, methanol as a solvent and titanium(IV) under 3 h reflux at 80 °C with sol thermal drying and calcination temperature of 450 °C. Further, the synthesis of size controlled SnO_2 NPs was demonstrated by optimizing the calcination temperature and molecular weight of polyethylene glycol (PEG, this is serving as chemical modifier reagent) using sol–gel method.[169] Results suggest that the size of SnO_2 NPs decreases with increasing molecular weight of PEG from 300 to 4000 and decreasing the calcination temperature from 600 °C to 450 °C.[169] Goncalves *et al.* demonstrated the one-pot synthesis of CdSe NPs using sol–gel method and realized quantum size effect in fabricated NPs, which is important for developing advanced optoelectronic devices.[170] Apart from them sol–gel is also a promising method for the synthesis of variety of NPs such as metal aluminate NPs, magnetic Fe–Co NPs, ZnO and Fe_2O_3 NPs, ZrB_2 NPs, $GdVO_4$ NPs, Ta_2O_5 NPs, *etc.*[171–176]

2.2.2 Microemulsion technique. Microemulsions can be defined as the thermally stable, macroscopically homogenous, optically transparent and isotropic dispersions constituting minimum of three components *i.e.*, polar phase (generally water), non-polar phase (generally hydrocarbon liquid or oil) and surfactant. Surfactant molecules creates the interfacial layer separating the aqueous and the organic phases, reduces the interfacial tension between the microemulsion and the excess phase and act as a steric barrier preventing the coalescence of the droplets.[177] Microemulsion system consists of monodispersed spherical droplets (diameter ranging from 600 nm to 8000 nm) of water-in-oil (w/o) or oil-in-water (o/w) depending on the surfactant used. The w/o reverse micellar system acts as an excellent reaction site for the NPs synthesis. Reverse micelle is water-in-oil microemulsion where the polar

head groups of the surfactant creating the aqueous core and resides towards inside whereas the organic tails of the surfactant molecules directed towards outside as shown in Fig. 9a.

In general there are two microemulsion routes to synthesize the NPs namely (1) one microemulsion method and the (2) two microemulsion method (Fig. 9b and c).[178] One microemulsion method can be further divided into two types *i.e.*, energy triggering method that needs a triggering agent to initiate the nucleation reaction within the single microemulsion containing the precursor and other is one microemulsion plus reactant method which is initiated by adding one of the reactant directly into microemulsion already carrying the second reactant (Fig. 9b). Malik *et al.* have reported the laser and radiolytically induced colloidal Au NPs formation in w/o microemulsion system with diameter ranging from 2.5–10 nm.[178] One microemulsion processes are diffusion controlled since the second trigger/reactant has to diffuse through the interfacial wall of the microemulsion encapsulating the first reactant to accomplish the NPs synthesis. In two microemulsion method, the two microemulsions carrying the separate reactants are mixed together in appropriate ratios (Fig. 9c). Brownian motion of the micelles helps them to approach each other resulting in intermicellar collisions and sufficiently energetic collisions leads to the mixing of the micellar components. Once both the reactant comes in a same micellar compartment, the chemical reaction takes place in this nanoreactor. As the critical number of molecules (N_{crit}) attained inside the micelle, it initiates the nucleation process and results in NPs formation. Numerous intermicellar collisions are needed for the sufficient reactant exchange, their mixing and finally their reaction to terminate at the end product.

Microemulsion technique was used most commonly for the synthesis of the inorganic nanomaterials including metal NPs (Au, Pt, Pd), semiconducting metal sulphite NPs (CdS, PbS, CuS, Cu_2S and CdSe), metal salt NPs ($BaCO_3$, $CaCO_3$ and $SrCO_3$), metal oxide NPs (ZrO_2, TiO_2, SiO_2, GeO_2 and Fe_2O_3), magnetic NPs ($(Mn,Zn)Fe_2O_4$, $(Ni,Zn)Fe_2O_4$, $ZnFe_2O_4$ and $BaFe_{12}O_{19}$) and composite NPs (CdS–TiO_2, CdS–ZnS, CdS–SnO_2). Metal NPs were easily prepared using microemulsion technique using the reduction strategy. Water-to-surfactant molar ratio (ω), type of continuous phase, metal ion concentration, type and concentration of the reducing agent, structure and amount of the surfactant used are some of the key parameters that control the metal NPs synthesis effectively.[177] Boutonnet *et al.* have used the reverse micelle microemulsion strategy to synthesize Pt, Pd, Rh and Ir NPs employing H_2PtCl_6, $Pd(NH_2)_4Cl_2$, $RhCl_2$ and $IrCl_3$, respectively as the precursors with hydrazine (N_2H_4) and active hydrogen as the reducing agent.[179] Solla-Gullon *et al.* have recently reported fast, easy and scalable production of Pt cubic NPs by reducing H_2PtCl_6 with sodium borohydride using w/o microemulsion process.[180] They revealed significant effect of introducing varying amount of HCl in the $H_2PtCl_6/NaBH_4$ microemulsion system in controlling the shape/surface of the Pt NPs. Zhang *et al.* have studied the synthesis of Ag NPs and also investigated the effect of ω (water/surfactant ratio) on the particle size and their size distribution.[181] Results revealed that there is continuous decrease in the particle size from ~5 nm to ~1.5 nm with reduction in the ω value from 15 to 2.5. They also investigated the effect of reducing agent concentration on the Ag NPs synthesis and leads to the fact that both less and excessive amount of reducing agent can hinder the synthesis process by affecting the stability of the colloids.[181] The same group have investigated the effect of increasing surfactant (sodium bis(2-ethylhexyl) sulfosuccinate; AOT) concentration on the Ag NP synthesis and observed reduction in the particle size with increasing surfactant amount.[182] Pileni *et al.* have introduced the synthesis of Cu NPs by reverse micelles using hydrazine as the reducing agent and revealed the effect of increasing water content in controlling the NPs size and the oxide content within the NPs structure.[183] CdS NPs were synthesized in AOT and triton reverse micelles with cadmium lauryl sulphate and cadmium AOT as the functional surfactant.[184] The diameter of the NPs is reported to be dependent on the relative composition of Cd^{2+} and S^{2-} ions. Chen *et al.* have accounted the synthesis of Ni NPs with average diameter of 4.7 nm using cationic w/o microemulsion of water/CTAB (cetyltrimethylammonium bromide)/*n*-hexanol system by the reduction of nickel chloride with hydrazine at an elevated temperature.[185] Subrata Kundu reported a novel methodology to synthesize shape-selective Au NPs by reduction of Au(III) ions with alkaline 2,7-dihydroxynaphthalene (DNP) in CTAB micellar media under 30 min continuous UV-irradiation.[186] The size and shape of the NPs were reported to be tuned by varying the Au(III) : CTAB molar ratio. Similar synthetic pathway was accounted to synthesize catalytically enhanced shape selective rhodium nanoparticles (Rh NPs) in the presence of DNP (reducing agent) and CTAB (surfactant) using 6 h UV-irradiation.[187] The growth of the NPs with different shapes (spherical, flower-like or cubic) was found to be directed by the surfactant-to-metal ion molar ratio and the concentration of DHN. Praharaj *et al.* also reported the size selective synthesis of Au NPs with average diameter from 9 nm to 15 nm in toluene

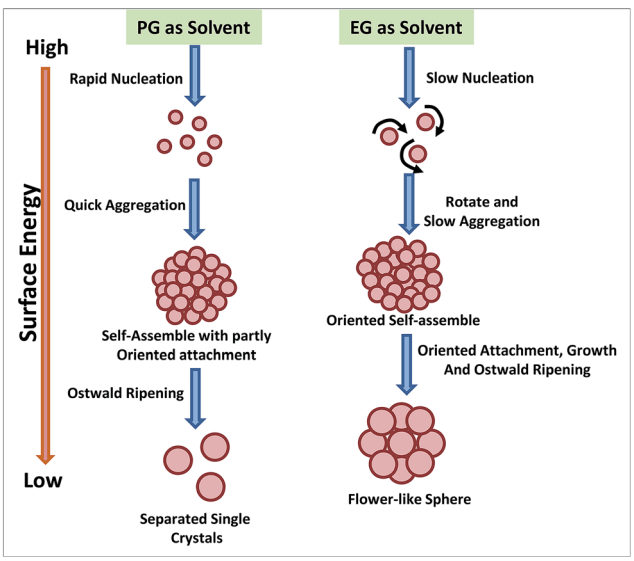

Fig. 10 The morphology evolution of iron oxide NPs in polyol processes using two different polyols. Adapted from ref. 225.

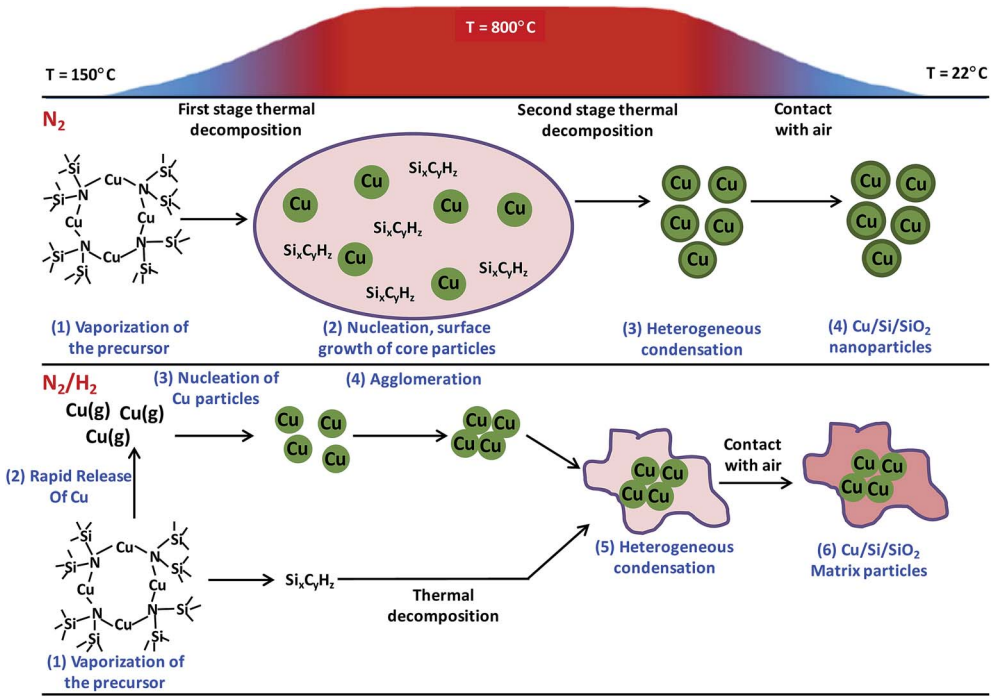

Fig. 11 Schematic representation of formation of Cu–Si/SiO_2 NPs by APCVS process. Reproduced with permission from ref. 233.

employing cationic surfactant of variable chain length.[188] Asher and co-workers developed and demonstrated a novel strategy to synthesize silica–CdS nanocomposites that allocate tailoring the size and morphology of the resultant NPs.[189] Gold–silver bimetallic NPs with varying mole fractions were synthesized in water-in-oil microemulsions of water/aerosol OT/isooctane system by co-reduction of $HAuCl_4$ and $AgNO_3$ with hydrazine.[190] Voucher *et al.* reported the preparation of crystalline NPs of hexacyanoferrate, cobalt pentacyanonitrosylferrate and chromium hexacyanochromate coordination polymers in water-in-oil microemulsions.[191] Mandal *et al.* reported the synthesis of bimetallic core–shell Pd–Au and Pd–Ag NPs of the size range of 10–30 nm using TX-100 micellar system by seed-mediated method.[192]

Microemulsion technique was not progressed much in term of designing organic NPs due to phase separation constraint and thus only few reports are available.[178] This method is known to be microemulsion polymerization when it comes to organic structures. Atik and Thomas reported first successful microemulsion polymerization in 1981 of latex NPs (average diameter: 20–35 nm) using CTAB/styrene/hexanol/water oil–water microemulsion coordination.[193] Three component microemulsion method was described to synthesize polystyrene NPs within size range of 20–30 nm using dodecyl trimethyl ammonium bromide (DTAB) and potassium persulphate (KPS) initiator.[194] Holdcroft and Guillet synthesized polystyrene NPs using pulse UV-triggered microemulsion polymerization.[195] Palani *et al.* studied the polymerization of MMA using MMA/ethylene glycol dimethacrylate/water system with acrylamide as amphiphile.[196] Organic NPs of cholesterol, retinol, Rhodiarome, Rhovanil were also been reported using different microemulsion systems including AOT/heptane/water, Triton/decanol/water, and CTABr/hexanol/water.[197] Microemulsion method was also been used to synthesize NPs of conducting polymers including polypyrrole, polyaniline, polythiophene, *etc.*[198–200]

2.2.3 Hydrothermal synthesis. This method is used to fabricate NPs of metal oxide, iron oxide and lithium iron phosphate keeping control over the characteristics of particles by varying the properties of near or supercritical water by using different pressure and temperature conditions. It can be performed in two types of systems, the batch hydrothermal or continuous hydrothermal process. The former is able to carry out a system with the desired ratio phases while the latter allows a higher rate of reaction to be achieved at a shorter period of time.[201]

In a chemical solution, NPs are produced from a colloidal system that consists of two or more phases (solid, liquid or gas states) of matter (*e.g.* gels and foams) mixed together under controlled pressure and temperature. The advantage of using this method includes the capability to synthesize a huge amount of NPs with an optimized size, morphology, composition and surface chemistry that is rationally inexpensive.[202] Du *et al.* reported the facile one-pot synthesis of Pt NPs using hydrothermal method and observed excellent electrocatalytic activity.[203] Ma *et al.* fabricated hydrophilic $NaYF_4$:Yb,Er NPs using this method and observed good bright upconversion luminescence. They suggested that these hydrophilic $NaYF_4$:Yb,Er NPs have great potential as luminescent labelling materials for biological applications.[204] This method was also used for the synthesis of NPs of oxides of iron, nickel and copper such as Fe_3O_4, α-Fe_2O_3, NiO, CuO, *etc.*[205–207] Hydrothermal is a facile and fast process for the synthesis of NPs of various other

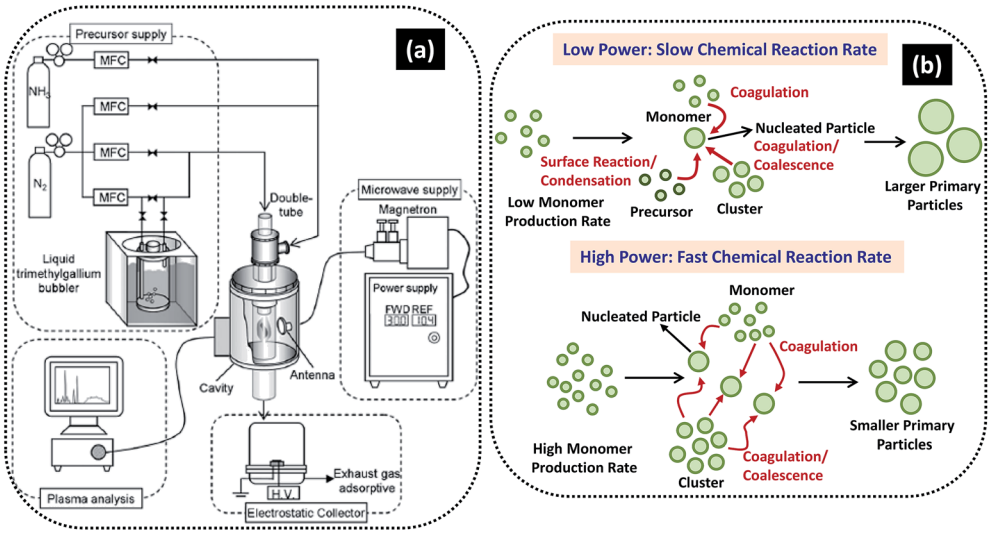

Fig. 12 (a) Schematic of MPECVD system and (b) possible mechanism of growth of NPs at low and high powers. Reproduced with permission from ref. 237.

materials such as $CoFe_2O_4$, Ag, $FeWO_4$, $La_{1-x}Sr_xCrO_3$, CdS, Zr, ZnO, *etc.*[208–214]

2.2.4 Polyol synthesis. Polyol process is the synthesis of metal-containing compounds using poly(ethylene glycol)s as the reaction medium, that plays a role of solvent, reducing agent and complexing agent at the same time, with dissolved stabilizing/protecting agents.[215] This chemical process was used to synthesize a wide range of metal based NPs (Ag, Pt, Pd, Pr, Cu), metal oxide NPs (ZnO, indium-tin-oxide; ITO, Gd_2O_3, Cu_2O), magnetic NPs and metal hybrid NPs. Xia *et al.* reported the synthesis of Pt NPs using polyol process at varying molar ratio of $NaNO_3$ and H_2PtCl_6.[216] They also reported the tailoring of size, morphology and crystallinity of NPs by slowing down the reduction of Pt(II) and Pt(IV) species (achieved by ethylene glycol) mediated by the varying concentration of nitrate ions in the solution which have a strong tendency to form stable complex with Pt(II) and Pt(IV). Moon *et al.* described the synthesis of spherical Cu NPs (diameter ~45 ± 8 nm) in the presence of poly(vinylpyrrolidone) as the protecting agent *via* polyol method.[217] Synthesis of spherical Ag NPs with controlled size (17± 2 nm) and high monodispersity was established using the polyol process.[218] They analyzed the effect of two varied polyol synthesis strategies, one dealing with the heating of the reaction medium having the precursor dissolved in it and other with heating the reaction medium receiving the precursor slowly using the injection method, on the NPs characteristics. Smaller silver NPs with more uniform size were obtained using the precursor injection method as compared to the precursor heating method.[218]

Xia *et al.* reported the synthesis of polycrystalline NPs of Cu_2O using copper nitrate, ethylene glycol and poly(vinyl pyrrolidone) as the precursor, reducing agent and the stabilizing agent, respectively.[219] Morphological transformation of these spherical Cu_2O NPs to nanocubes was observed by introducing NaCl in the reaction mixture which is explained by the fact that the added Cl^- ions play a role in retarding the reduction kinetics, stabilizing the {100} plane of the Cu_2O crystals that inducing the formation of single-crystal nanocubes, which can grow in size *via* Oswald ripening. Low temperature synthesis of ITO NPs was carried out by Jeyadevan and coworkers in polyols and alcohols including ethylene glycol, trimethylene glycol and 1-heptanol.[220] The NPs characteristics were found to be influenced by the type of polyol used as the reaction medium. In another work, Moon *et al.* reported the preparation of ZnO NPs by polyol method and showed that the amount of water and way of precursor addition affects the characteristic of the NPs immensely.[221] Similarly, the polyol synthesis method was also used to synthesize NPs of Gd_2O_3 and Pr_6O_{11}.[222,223]

Polyol process was also employed for developing low temperature strategies to synthesize magnetic NPs of magnetite, Fe_3O_4, *etc.*[224,225] Cheng *et al.* have very nicely described the effect of two different polyols (ethylene glycol; EG and 1,2-propylene glycol; PG) having different reduction capability on the morphology evolution of the Fe_3O_4 magnetic NPs (Fig. 10).[225] Due to the higher reductive ability of PG, there is faster formation and growth rate for the NPs leads to Fe_3O_4 aggregation and generation of more misaligned mesocrystals. In the mesocrystal, the neighbouring NPs merge together and finally integrate into a single crystal with a porous structure during the Ostwald ripening process. However, due to relatively lower NP formation rate in EG, most of the particles got enough time to self-assemble along the same orientation in the cluster. Each cluster, with its highly ordered arrangement of NPs, can be regarded as a single mesocrystal. And this mesocrystal can retain its secondary structure owing to the lower surface energy. This one-pot facile chemical process can also be used to design hybrid metal NPs including $CoSb_3$, FeCo, *etc.*[226,227]

2.2.5 Chemical vapour deposition (CVD) & chemical vapour synthesis (CVS). CVD is a process, which is often used

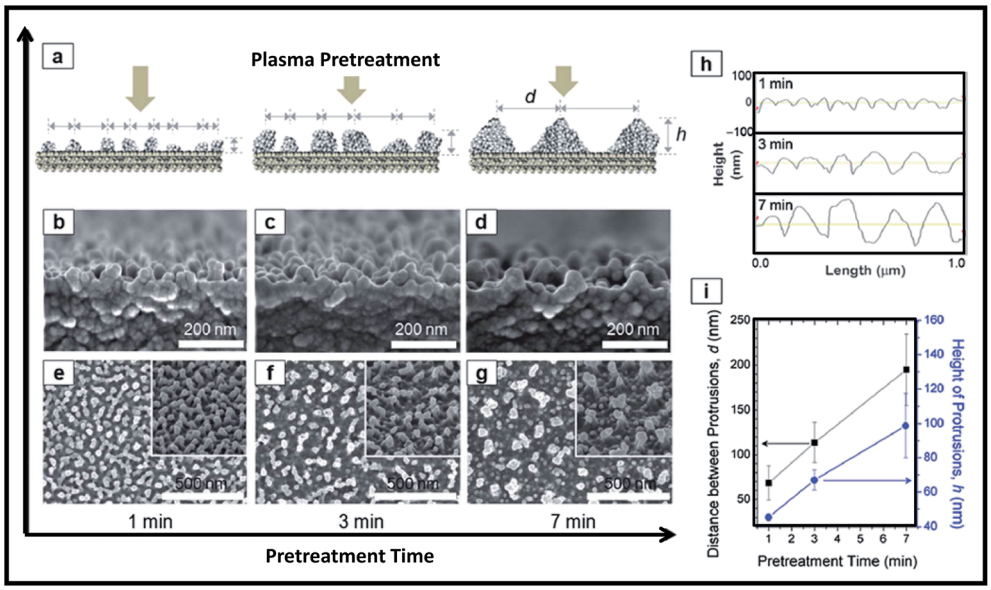

Fig. 13 Plasma pre-treatment for creation of polymer protrusions. (a) Schematic diagram and (b–d) cross section as well as (e–g) plane view FE-SEM images showing the effect of treatment time on aspect ratio of formed polymer protrusions. (h) AFM line profiles and (i) the corresponding quantitative data of the protrusions (h and d) with plasma treatment times. Reproduced with permission from ref. 247.

for the deposition of solid films from vapour phase *via* chemical reactions occurring at very high temperature condition. Thin films produced by CVD process at certain conditions also contain ultrafine particles. Hence, the synthesis of NPs can also be possible by this method if the CVD system is modified/optimized for the conditions given below:

(i) High temperatures (in hot wall reactors)

(ii) High supersaturations (high partial pressure of monomers at a low vapor pressure of the bulk solid)

(iii) Long residence times (low gas flows or long reactors)

(iv) Small substrates

Hence, when the process conditions adjusted in such a way that CVD process produces NPs instead of thin solid films, then the modified process is called as CVS. The process CVS also termed as chemical vapor reaction (CVR), chemical vapor precipitation (CVP) and chemical vapor condensation (CVC). In this synthesis method, the precursors that exist in the three different states (solid, liquid, gas) are produced in the form of vapour in the reactor under an environment that requires particles to undergo the process of nucleation. In addition, CVS forms multi-component or doped NPs by the use of a variety of precursors. For instance, erbium (Er) had been incorporated into Si NPs by the use of precursors such as the organometallic erbium and disilane compound, and composite NPs are produced by encapsulating a material within the other (*e.g.* silicon tetrachloride in reaction with sodium chloride that result in the formation of sodium chloride-encapsulated silicon particles).[228] CVS method has been extensively utilized for the synthesis of NPs using a variety of materials including ZnO, WS_2, iron oxide, copper and silicon oxides, Al doped ZnO, fluorine doped tin oxide, Cr doped ZnO, *etc.*[229–236] Polarz *et al.* synthesized size selected ZnO NPs (6–30 nm) by CVS process using the tetrameric alkyl-alkoxy zinc compound $[CH_3ZnOCH(CH_3)_2]_4$ as the precursor, which was chemically transformed into ZnO through gas-phase reactions.[229] Hartner *et al.* synthesized Al doped ZnO (AZO) NPs by CVS process using diethylzinc (DEZn) and triethylaluminum (TEAl) as precursors for Zn and Al, respectively, while He gas was chosen as carrier gas.[230] Oxygen gas with constant flow rate of 1000 sccm was inserted in alumina tube with an inner diameter of 19 mm, and temperature and pressure of the system was kept at 1073 K and 20 mbar, respectively. With these conditions, high quality AZO NPs were synthesized and their particle size was found to decrease with increasing the Al concentration. In comparison to other processes, CVS process has following advantages for the synthesis of AZO NPs:

(i) In contrast to wet synthesis, CVS process allows high percentage of Al doping in ZnO

(ii) CVS process can produce NPs at higher growth rate, leading to reduction of the cost of the material

(iii) CVS produced AZO NPs with high crystallinity

(iv) Unlike other chemical process, CVS process avoids the use of additional step which is the removal of organic contaminant after the synthesis

Jin *et al.* reported the synthesis of Cr doped ZnO (CZO) NPs using CVS process.[231] Their CVS system was splitted into two zones for evaporation and subsequently pyrolysis of the precursors. Zinc acetylacetonate ($Zn(acac)_2$) and chromium acetylacetonate ($Cr(acac)_3$) were used as precursors for the synthesis of CZO NPs. These precursors were evaporated from alumina boat at low temperature first zone and then transported through He carrier gas into high temperature second zone for pyrolysis and oxidizing at 1173 K. It should be noted that the temperature in first zone was kept at 493 K for pure ZnO NPs, and changed to 423 K for CZO NPs. The crystallographic and microscopic analysis revealed that the size of pure ZnO NPs

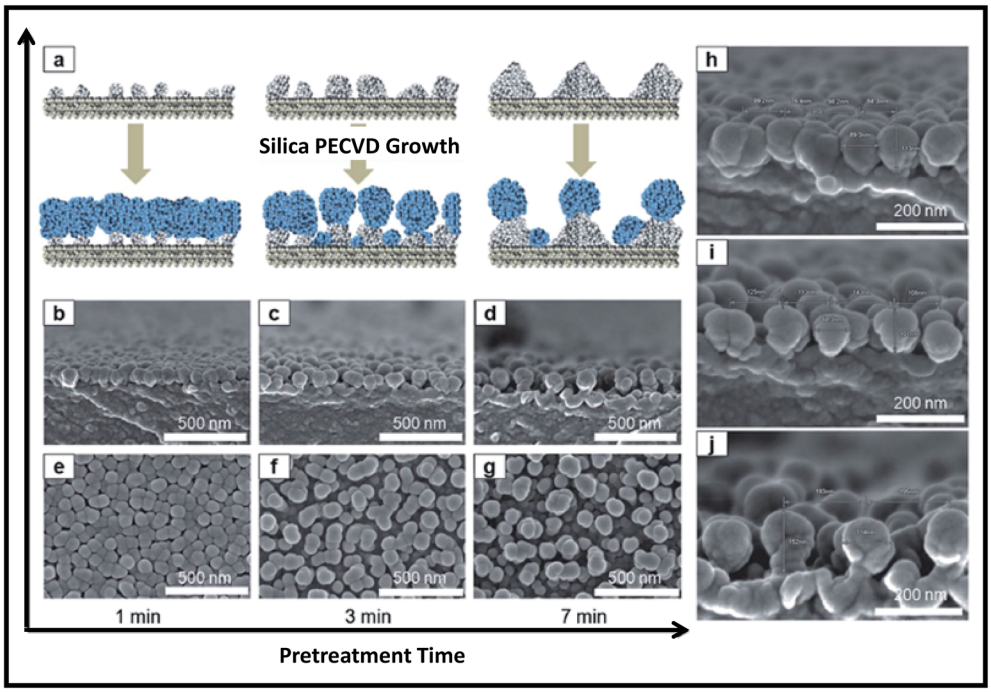

Fig. 14 (a) Schematic showing the role of pre-treated polymer surfaces on the synthesis of silica NPs. (b–d) Cross-sectional and (e–g) plane view FE-SEM images of silica NPs formed on pre-treated polymer surfaces. (h–j) High magnification cross-sectional FESEM images of silica NPs formed on pre-treated polymer surfaces for different treatment times of (h) 1 min, (i) 3 min, and (j) 7 min. Reproduced with permission from ref. 247.

was ~19 nm, which was decreased to ~6 nm in case of CZO NPs with Cr concentration of 6 at%. Suffner *et al.* demonstrated the synthesis of fluorine doped SnO_2 (FTO) NPs using CVS method.[232] Tetramethyltin (TMT) and difluoromethane (DFM) were used as the precursors, while oxygen and helium were used as the reactive and carrier gases, respectively, for the synthesis of FTO NPs. The flow rate of TMT, oxygen and helium was kept constant at 25 sccm, 1500 sccm and 150 sccm, respectively, while it was changed from 0 to 1.5 sccm for DFM in order to synthesize pure tin oxide (TO) NPs and FTO NPs. The chemical reactions for the synthesis of these NPs occurred at temperature and pressure of 1200 °C and 15 mbar, respectively. When synthesized at DFM flow rate of 1.5 sccm, size of FTO NPs were found to be in the range of 3 to 10 nm. The synthesized ZnO, AZO, CZO and FTO NPs can find wide electronic and optoelectronic applications.

Using atmospheric pressure CVS (APCVS) process, Lahde *et al.* reported the synthesis of Cu NP composite in an amorphous silicon dioxide (a-SiO_2), where Cu NPs were either coated with a-SiO_2 or embedded in a-SiO_2 matrix.[233] In order to prepare NP composite structure using APCVS, first step was to synthesize metal–organic precursor. They synthesized metal–organic precursor $[CuN(SiMe_3)_2]_4$, also called as Cu(I), using standard process. The ARCVS system, which was used for synthesis of NP composite, included different zones such as:

(i) Precursor feeding zone
(ii) Heating zone
(iii) Dilution and cooling zone
(iv) Sampling and particle collection zone

Using a heat bath, the synthesized Cu(I) precursor was vaporized at temperature between 100 and 250 °C. The pre-heated (100–250 °C) pure nitrogen or a mixture of hydrogen (10% v) and nitrogen was used as carriers, while the flow rate was kept to be 0.3 L min^{-1}. After this, precursor vapor was transported to heating zone of system and mixed with nitrogen at flow rate of 1.8 L min^{-1} at temperature 800 °C. However, at the exit point of the heating zone the aerosol was diluted with nitrogen at the flow rate of 10.4 L min^{-1} to quench the particle. Finally, the particle sampling and collection was done from the gas phase. Inclusion of hydrogen in nitrogen gas significantly affected the structure of NP composite. In pure nitrogen atmosphere the Si/SiO_2 protective coating was formed around the Cu NPs. While in mixed hydrogen/nitrogen environment, the Cu NPs were embedded in SiO_2 matrix. Schematic showing the mechanism of formation of NP composite in pure nitrogen and mixed nitrogen/hydrogen atmosphere is depicted in Fig. 11.

Further Lee *et al.* reported the fabrication of fullerene-like WS_2 NPs using CVS process.[234] The $W(CO)_6$ was used as precursor for tungsten (W), which was decomposed in the temperature between 420 and 1000 °C. The evaporation temperature was varied from 80 to 110 °C at flowing He gas with varied flow rate from 2000 cm^3 min^{-1} up to 4000 cm^3 min^{-1}. In order to form WS_2 NPs, the decomposition of tungsten hexacarbonyl $W(CO)_6$ was performed in the presence of sulphur vapour with their partial pressure varied from 0.02 to 0.04 atm. Finally, at optimized conditions, the CVC process produces fullerene-like WS_2 NPs having mean particle size in the range from 20 to 70 nm.

Table 4 Various microorganisms reported to be involved in the synthesis of different types of NPs[a]

Microorganism		Type of nanoparticles	Size of nanoparticles	Mode of synthesis	Reference
Bacteria	*Staphylococcus aureus*	Ag NPs	160–180 nm	Extracellular	255
	Bacillus cereus	Ag NPs	4–5 nm	Extracellular	258
	Marinobacter pelagius	Au NPs	2–10 nm	Extracellular	260
	Actinobacter sp.	Au NPs	50–500 nm	Extracellular	279
	Enterobacter sp.	Hg NPs	2–5 nm	Intracellular	280
	Lactobacillus	TiO_2 NPs	40–60 nm	Extracellular	257
	Escherichia coli	CdS QDs	2–5 nm	Intracellular	259
	Escherichia coli	CdTe QDs	2–3.2 nm	Extracellular	281
Fungi	*Verticillium*	Ag NPs	25 ± 12 nm	Intracellular	261
	Aspergillus terreus	Ag NPs	1–20 nm	Extracellular	262
	Bryophilous Rhizoctoni	Ag NPs	20–50 nm	Extracellular	263
	Aspergillus flavus	Ag NPs	8.92 ± 1.61 nm	Extracellular	264
	Pleurotus ostreatus	Ag NPs	8–50 nm	Extracellular	265
	Fusarium oxysporum	Au NPs	8–40 nm	Extracellular	282
	Fusarium oxysporum	SiO_2 NPs	2–4 nm	Extracellular	268
	Fusarium oxysporum	Magnetite NPs	20–50 nm	Extracellular	269
	Fusarium oxysporum	TiO_2 NPs	6–13 nm	Extracellular	270
	Fusarium oxysporum	ZrO_2 NPs	7–8 nm	Extracellular	271
Yeast & actinomycetes	*MKY3*	Ag NPs	2–5 nm	Extracellular	272
	Candida albicans	Au NPs	20–40 nm	Extracellular	266
	Hansenula anomala	Au NPs	14 nm	Extracellular	273
	Yarrowia lipolytica NCIM 3589	Au NPs	9–23 nm	Extracellular	274
	Candida glabrata	CdS NPs	2 nm	Intracellular	275
	Rhodosporidium diobovatum	PbS NPs	2–5 nm	Intracellular	276
	Thermomonospora sp.	Au NPs	8–40 nm	Extracellular	277
	Rhodococcus sp.	AuNPs	5–15 nm	Intracellular	283

[a] Abbreviations: NPs – nanoparticles, QDs – quantum dots.

CVS process was also used widely for the synthesis of iron oxide NPs of mean particle size from 80–90 nm and various other metal oxide NPs.[235,236]

2.2.6 Plasma enhanced chemical vapour deposition (PECVD). Plasma enhanced chemical vapour deposition, also called as plasma assisted chemical vapour deposition (PACVD), is a popular CVD process which is widely used for the deposition of thin films. PECVD process can also be used for the synthesis of NPs. As the name suggests, plasma enhances the chemical reactions for the synthesis of thin films and NPs. PECVD unit mainly includes: (1) vacuum processing system, (2) gaseous precursors, (3) power supply (AC or DC) and (4) heater. Unlike usual CVD process, the synthesis of thin films and NPs by PECVD takes place at comparatively lower temperature. As the plasma is partially ionized gas, ionized species and radicals participate in growth of thin films and NPs. Synthesis of NPs of several types of materials was demonstrated by PECVD. Shimada *et al.* reported the synthesis of gallium nitride (GaN) NPs by microwave plasma enhanced chemical vapour deposition (MPECVD).[237] Schematic of the MPECVD system is shown in Fig. 12a. For the synthesis of GaN NPs, trimethylgallium (TMG) was used as a precursor for Ga, while nitrogen and ammonia (NH_3) were used for nitridation. Various parameters such as antenna length, power and operating pressure were varied to optimize the input parameters. Using 5×10^{-4} vol% TMG at operating pressure of 20 kPa, the decrease in size of GaN NPs with increase in microwave power was demonstrated. Average particle size of 7.3, 5.6 and 5.2 nm was achieved using microwave powers of 800, 1000, 1200 W, respectively.

The mechanism involved in the synthesis of NPs of varied sizes is depicted in Fig. 12b. At low input power, the plasma reactivity remains low causing slow chemical reaction rate and hence, results in the formation of monomers. Because of slow reaction rate, relatively small number of nuclei are formed and at the same time significant amount of unreacted precursor molecules exit. When large numbers of unreacted species condense and react with relative small number of nuclei, the size of the resulting particles becomes larger. However, at higher power the plasma reactivity and chemical reaction got enhanced, leading to formation of more nuclei and disappearance of unreacted species. Under this condition the coagulational growth can be prevented and formation of small size NPs would be possible. Thus, the size of GaN NPs can be efficiently controlled by the input power. Dwivedi *et al.* used PECVD method to synthesize hard carbon nanoparticle based films by tuning the self-bias, introducing different doping strategies and using metal/carbon bi- and multilayer designs; where nitrogen was used as foreign atoms while Ti, Cu and Ag were used as metal layer in metal/carbon bi- and multilayer structures.[238–244] Designed carbon nanoparticles films showed excellent electrical, field emission, optical and mechanical properties with potential applications in the field of emission devices, protective coatings, solar cells, *etc.*

The synthesis of carbon NPs and hydrogenated Si NPs was also reported by MPECVD and radio frequency PECVD (RF-

Table 5 Self-assembled nanoclusters of different nanoparticles synthesized using DNA as template or scaffold[a]

Self assembled nanocluster of	Shape of nanocluster	Dimensions	Applications	References
Ag NPs	Wire like	$\phi_P = 17 \pm 3$ nm, IPD $= 1.7 \pm 0.2$ nm	As ultrasensitive SERS substrate	285
Os NPs	Wire like	$\phi_P \sim 2 \pm 0.5$ nm, $\phi_W \sim 290 \pm 20$ nm	Catalysis and SERS	298
	Honeycomb like	$\phi_P = 1.5 \pm 0.2$ nm, $\phi_W = 400$ nm		
Os NPs (organosol)	Wire like	$\phi_P = 2.6 \pm 0.2$ nm, $L = 0.54 \pm 0.03$ μm	Catalysis and SERS	289
	Aggregated wires	$\phi_P = 1.2 \pm 0.2$ nm, $L =$ 8–10 micron		
ZnO NPs	Wire-like	$\phi_P = 150 \pm 15$ nm, $L =$ 1–2 μm	Catalysis and dye-sensitized solar cells	288
	Flower-like	$\phi_P = 350 \pm 50$		
	Flake-like	$\phi_P = 80 \pm 10$ nm		
β-MnO_2 NPs	Wire-like	$L = 1.9 \pm 0.2$ mm, $\phi_P = 35 \pm 5$ nm	Catalysis and supercapacitor	299
	Flake-like	$L = 275 \pm 25$ nm, $\phi_P = 25 \pm 5$ nm		
TiO_2 NPs	Wire like cluster (large)	$\phi_P = 15 \pm 5$ nm, $\phi_C = 180 \pm 20$ nm	Supercapacitor and dye sensitized solar cells	300
	Wire like cluster (small)	$\phi_P = 10 \pm 2$ nm, $\phi_C = 40 \pm 5$ nm		
$NiWO_4$ NPs	Chain like (small)	$L = 2 \pm 0.2$ μm, $\phi_C = 175 \pm 15$ nm, $\phi_P = 20 \pm 5$ nm	Catalysis and supercapacitor	291
	Chain like (large)	$L = 3.4 \pm 0.2$ μm, $\phi_C = 245 \pm 15$ nm, $\phi_P = 26 \pm 4$ nm		
$ZnWO_4$ NPs	Aggregated, chain like	$\phi_P = 75 \pm 5$ nm, $\phi_C = \sim 75 \pm 15$ nm, $L = \sim 3$ μm	High performance supercapacitor and catalysis	292
$MnWO_4$ NPs	Wire-like	$\phi_P = 75 \pm 15$ nm, $L \geq 700$ nm	Magnetic, catalysis and supercapacitor studies	293
	Flake-like	$L =$ 90–180 nm		
	Rice-like	$L = 90 \pm 10$ nm, ϕ_P 25 $\pm$ 5 nm		

[a] Abbreviations: AgNPs – silver nanoparticles, NPs – nanoparticles, ϕ_P – particle diameter, ϕ_C – chain diameter, ϕ_W – wire diameter, L – chain length, SERS – surface enhanced Raman spectroscopy.

PECVD) techniques, respectively.[245,246] Yun *et al.* demonstrated the synthesis of silica NP array on flexible polymer substrate using PECVD process involving following two steps:[247]

(i) Pre-plasma treatment of polymer surface followed by

(ii) Coating of silica NPs array

To perform plasma pre-treatment, the polymer substrate (polyethylene terephthalate; PET) was placed on electrode housed in vacuum system (base pressure of 6.7 Pa). The plasma pre-treatment was performed on PET at constant RF power of 200 W (1.1 W cm^{-2}), working pressure of 22.7 Pa and Ar flow rate of 50 sccm, while the plasma treatment time was varied. The Ar plasma pre-treatment of the PET surfaces led to the formation of polymer protrusions due to morphological modifications of polymer chains as shown in Fig. 13. Height of protrusions (h) and the distance between neighbouring protrusions (d) was found to increase continuously with increasing pre-treatment time from 1 min to 7 min (Fig. 13). Subsequently silica NPs are deposited on pre-treated polymer surfaces by plasma polymerization of hexamethyldisiloxane (HMDSO). First in evaporator, the vapors of HMDSO are formed by thermal evaporation of precursor liquid HMDSO at a heating temperature of 130 °C and then they are mixed with O_2 and Ar gases at a flow rate ratio of HMDSO : O_2 : Ar = 1.8 : 10 : 100 before entering into the synthesis chamber. Finally silica NPs are grown having O : Si atomic ratio of 1.9–2.0. Fig. 14 shows the growth of silica NPs on pre-treated polymer surfaces.

Of note, plasma pre-treatment time of polymer surfaces significantly affects the growth of NPs. As the polymer protrusions reduce with increasing plasma pre-treatment time, the density of the formed silica NPs also reduces with increasing plasma-pre-treatment time. The globular silica NPs synthesized by this method showed excellent antireflective property.

2.2.7 Chemical methods for the synthesis of graphene oxide nanoparticles. Recently, graphene oxide nanostructures received wider attention owing to their multiple applications including drug delivery, catalysis, cell therapy, environmental monitoring, biosensors, field emission transistors, clean energy devices, *etc.*[248] Considering their broad range applicability, this section on the synthesis of graphene oxide nanoparticles (GON) has been included here to enhance the comprehensiveness of the present review. In most of the reports available, modified Hummers methods have been used to synthesize GON of varied sizes.[249] Zhao *et al.* adopted modified Hummers method to synthesize nearly spherical GON with nearly monodisperse size of 43.36 ± 8.42 nm from graphite powder.[250] Authors have further functionalized the GON with cystamine modified PEGylated alginate to design drug delivery platform for tumour microenvironment-responsive triggered release of doxorubicin. Jana *et al.* synthesized Tris (nitrilo tris-acetic acid), Tris-NTA, functionalized GON using modified Hummers method with average particle size of 213 nm which can reconstitute kinesin mediated intracellular cargo transport and can deliver multiple proteins and therapeutic antimitotic dodecapeptide peptides into the cancer cell.[251] Authors used similar strategy to fabricate dual functionalized GON employing Tris-NTA and biotin for cellular delivery of oligohistidine – and biotin-tagged

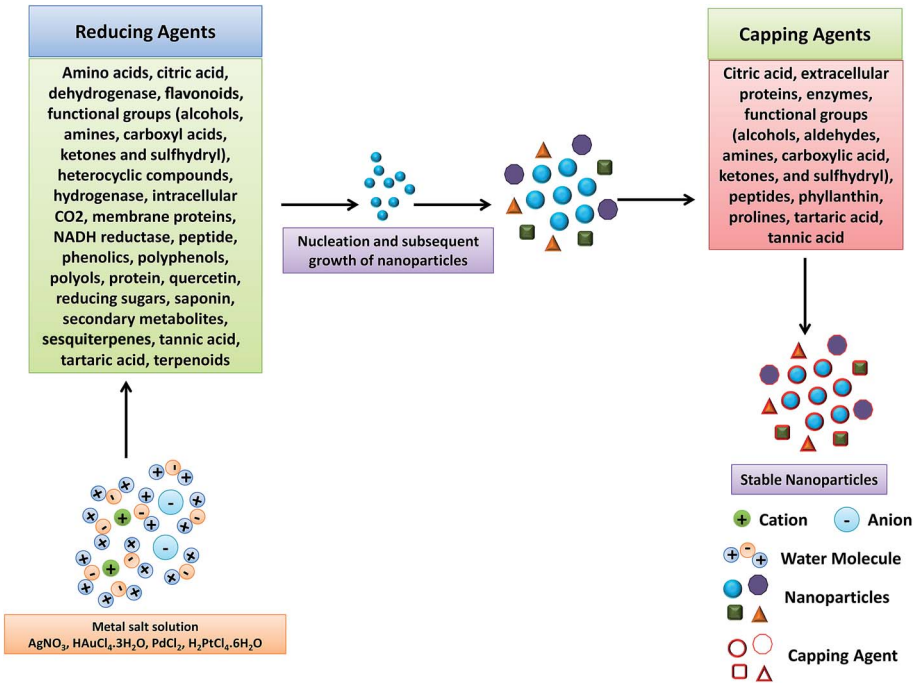

Fig. 15 Mechanism for the biogenic synthesis of metal NPs using plant extract. Reproduced with permission from ref. 305.

biomolecules.[252] Lee *et al.* reported the synthesis of GON with the size of 30 nm by first exfoliating graphite into graphene oxide using modified Hummer method followed by their ultrasonication.[253] These tiny GON have been shown to be applicable as non-bleaching optical probe for two photon luminescence imaging and cell therapy.

2.3 Bio-assisted methods for the synthesis of nanoparticles

Bio-assisted methods, biosynthesis or green synthesis provides an environmentally benign, low-toxic, cost-effective and efficient protocol to synthesize and fabricate NPs. These methods employ biological systems like bacteria, fungi, viruses, yeast, actinomycetes, plant extracts, *etc.* for the synthesis of metal and metal oxide NPs. Bio-assisted methods can be broadly divided into three categories:

(i) Biogenic synthesis using microorganisms
(ii) Biogenic synthesis using biomolecules as the templates
(iii) Biogenic synthesis using plant extracts

2.3.1 Biogenic synthesis using microorganisms. Prokaryotic bacteria, actinomycetes, fungi, algae and yeast are extensively used as bio-reactors for the synthesis of NPs. Enormous scientific efforts were made to develop this strategy of producing a variety of NPs (Ag, Au, Pd, TiO_2, CdS, *etc.*). Microorganisms grab target ions from their environment and then turn the metal ions into the element metal through enzymes generated by cellular activities. This synthesis can be classified into intracellular and extracellular depending upon the location of NP synthesis. The intracellular method involves transporting of metal ions into the microbial cell to form NPs in the presence of enzymes. The extracellular synthesis of NPs involves trapping of metal ions on the surface of the cells and reducing ions in the presence of enzymes.[254] Bacteria utilize a number of anionic functional groups, proteins and enzymes, reducing sugars, *etc.* in bacterial biomass to reduce interacting metal ions. Bacterium *S. aureus* was used for the extracellular synthesis of bioactive Ag NPs with antimicrobial activities.[255] Boon *et al.* described non-enzymatic production of Ag NPs using biomatrix of the bacteria both as the reducing and the capping agent.[256] The presence of anionic functional group rich cell wall around the Gram-positive bacteria constituting of peptidoglycan, teichoic acids, lipoteichoic acids, proteins, and polysaccharides acts as sites for the biosorption and subsequent reduction of silver cations. Lactobacillus bacterium was used as the biofactories for the synthesis of TiO_2 NPs with size ranging from 40–60 nm.[257] Gunasekaran *et al.* reported the isolation of new hyper metal resistant *Bacillus cereus* PGNI bacterial strain that form intracellular crystalline Ag NPs.[258] Bacterial system was also employed to synthesize semiconducting CdS nanocrystals (wurtzite crystal structure).[259] In another interesting report, authors explored the potential of marine bacteria for the production of AuNPs.[260]

Fungal-mediated green chemistry approach for the synthesis of NPs has many advantages like higher bioaccumulation, economic viability, easily scaled up synthesis method due to simple downstream processing and biomass handling. In this context, Mukherjee *et al.* demonstrated a fungal-assisted biological method to synthesize silver NPs using fungus *Verticillium*.[261] Exposure of the fungal biomass to the aqueous Ag^+ ions leads to their intracellular reduction to silver NPs of dimension 25 ± 12 nm. Microscopic investigation reveal mycelia surface as the predominant site for the NPs synthesis which is mediated by the enzymes available on the mycelia cell

Table 6 Key nanoparticles and their important applications in various scientific fields

Nanoparticles	Possible key applications
Ag	Nanomedicines: antibacterial agent (healthcare, food technology, textile coating, environmental cleaning, water disinfection),[321] wound healing,[322,323] cancer therapeutics[324] Diagnosis: designing highly sensitive biosensor electrodes/chips,[325] biological tagging for quantitative detection[326] Solar cells,[327] electroluminescent displays,[328] optical sensors, surface enhanced Raman spectroscopy[99,285,329] To generate eco-friendly electrical contacts for electrical devices[330] Supercapacitors[93] Catalysis[331,286]
Au	Nanomedicines: drug and gene delivery,[332] hyperthermia-assisted cancer phototherapy,[333,334] photodynamic therapy[335] Biosensors: highly sensitive optical,[336] electrochemical[337] and plasmon resonance biosensors[338] Sensors[90] *Ex vivo* and *in vivo* bio-imaging:[339] two photon luminescence imaging, magnetic resonance imaging, photoacoustic tomography, Raman imaging, *etc.* Antibacterial agents[340] Solar cells,[341] energy storage devices[90]
Fe	Biomedical applications: biosensors,[342] MRI contrast enhancement,[343] hyperthermia[344] Magnetic and electrical applications: magnetic recording media, soft magnetic materials, motors Catalytic applications
Pt	Biomedical applications: affinity probe for the detection of small biomolecules,[345] catalytic nanomedicines,[346] biosensors[347] Catalysis[348] Solar cells[349]
Pd	Surface enhanced Raman scattering and electrocatalysis[350] Catalysis[351] Antibacterial activity[352] Fuel cells[353] Biosensors[354]
Ge	Electronic/optoelectronic[82]
CeO_2	Potential regenerative antioxidant[355] Therapeutic applications for reactive oxygen species (ROS)-related diseases *e.g.* cancer, diabetes, arthritis, infertility, macular degeneration[356,357] Catalytic convertor for removing toxic gases[355] Solid oxide fuel cells[355] Biosensors[358] Photocatalysis[125] Antibacterial activity[359]
TiO_2	Drug delivery[321,360] For cell delivery[361] Antimicrobial coatings As UV filters in sunscreens,[362] toothpaste, cosmetics, *etc.* Biosensors[363]
ZnO	Solar cells[364] Photocatalytic and hygienic coatings[365] Biosensors[366] Important additive for different cosmetics, ointments and food products Cure activator for rubbers of different kinds[367] Antibacterial[65]
Fe_2O_3	Due to its excellent magnetic properties, they are being used in magnetic seals and inks, magnetic recording media, catalysts, and ferrofluids[368] Development of immunoassays, magnetic resonance imaging contrast agents, and targeted drug delivery vehicles, as well as in magnetic hyperthermia[369]
CdS	As fluorescent probes[370] Optical, electrochemical and photoelectrochemical biosensors[371,372] Solar cells[373] Photoluminescence devices[374]
CdSe	Solar cells[338,375] Light emitting diodes[339,376]
Magnetic nanoparticles	Biomedical applications: gene delivery,[377] magnetic resonance imaging,[378] magnetic carriers for bio-separation[379] Catalyst supports[380]

Table 6 (*Contd.*)

Nanoparticles	Possible key applications
Upconversion (lanthanides) nanoparticles	*In vivo* cell imaging[381] Near-infrared photodynamic therapy[382] Light nanotransducers for photoactivation applications[383] Solar cells[384]
Carbon nanoparticles	Cancer diagnostic and therapy[385,386] Antibacterial[387] Lithium sulfur batteries[388] Designing of fluorescent imaging probes[389] Catalysis[62] Solar cells, protective coatings and emission devices[238–244]
Graphene oxide nanoparticles	For cell delivery[248,251,252] In drug delivery for cancer therapeutics[390] Non-bleaching optical probe for two-photon luminescence imaging[253] Cell therapy[253] Biosensors[391]
Polymeric NPs	Nanomedicines and drug delivery[392–394] Fluorescent polymeric NPs for cell imaging[395] Photoacoustic imaging[396] Biosensors[200]

wall. Biosynthesis of Ag NPs was also reported using *Aspergillus terreus* fungus and herein the speculated mechanism is reported to be NADH dependant enzyme catalyzed extracellular reaction process.[262] There are number of other reports available on the biosynthesis of Ag NPs using versatile fungal species including *Pleurotus ostreatus*, *Aspergillus flavus*, *Bryophilous Rhizoctoni*, *etc.*[263–265] Chauhan and co-workers synthesized Au NPs (20–40 nm) employing *Candida albicans* mediated bioreduction strategy.[266] The mechanism of fungal biosynthesis of Au NPs is very well explained by Kitching *et al.*[267] Bansal *et al.* demonstrated the biotransformation of amorphous silica in cheap agro-based rice husk to nanocrystalline silica (2–6 nm).[268] There are several reports on the NPs biosynthesis of magnatite, TiO_2 and ZrO_2 using various fungal species.[269–271]

Yeast and actinomycetes also established their applicability for the bio-inspired synthesis of NPs. Yeast is an eukaryotic microorganisms belonging to the fungi kingdom. Kowshik *et al.* reported bulk extracellular synthesis of silver NPs (2–5 nm) using silver tolerant yeast strain *MKY3*.[272] Kandasamy *et al.* shown the applicability of *Hanensula anomala* species to reduce gold salt generating AuNPs.[273] *Yarrowia lipolytica* was also reported as efficient reducing agent for $AuCl_4$ to produce gold NPs.[274] Carboxyl, hydroxyl and amide groups on the cell surface are anticipated to be responsible for AuNPs synthesis. Yeast was also reported to be useful in the synthesis of Cd and PbS NPs using *Candida glabrata* and *Rhodosporidium diobovatum* species, respectively.[275,276] Enriched with various enzymes, actinomycetes have been for the reduction of $AuCl_4^-$ to generate Au NPs (8 nm) by *Thermomonospora* sp.[277] Torres-Chavolla *et al.* reported the synthesis of comparatively larger monodispersed Au NPs (30–60 nm) in the presence of *Thermomonospora curvata*, *Thermomonospora fusca* and *Thermomonospora chromogena* species.[278] Table 4 lists various NPs synthesized using a variety of microorganisms.

2.3.2 Biomolecules as templates to design nanoparticles. Various biomolecules like nucleic acids, membranes, viruses and diatoms were used as templates to synthesize NPs. DNA is widely known as an excellent biomolecular template that has a strong attraction with transition metal ions. It was shown that DNA hydrogel could be made and crosslinked before incorporating transition metal ions (*e.g.* gold, Au(III) metal ions) to DNA macromolecules that eventually lead to the formation of Au NPs. The process involves a reduction of Au(III) leading to the formation of Au atoms and metal clusters that develop into Au NPs on the chain of DNA.[284] Kundu *et al.* reported the synthesis of wide variety of NPs and nanoparticles assemblies using DNA as the templates or organic scaffolds.[285–300] They accounted a DNA-mediated strategy to synthesize highly stable wire-like clusters of Ag NPs with average particle size of the 17 ± 3 nm and inter-particle gap of $\sim 1.7 \pm 0.2$ nm for their potential applicability as ultrasensitive SERS substrates.[285] These Ag NPs assemblies grown over DNA chains have also been shown to possess good catalytic activity towards the reduction of aromatic nitro compounds.[286] An electroless, photolytic, DNA-mediated method was described to synthesize gold nanoclusters (10–40 nm) and continuous long nanostructures (diameter: 40–70 nm) with the nanostructures exhibiting resistivity equivalent to the pure metals.[287] In another report, authors demonstrated synthesis strategy to design shape-sensitive ZnO nanoparticles with various morphologies (wire-like, $\sim 150 \pm 15$ nm; flake like, $\sim 80 \pm 10$ nm; flower like, $\sim 350 \pm 50$ nm) using DNA as biotemplate for dye sensitized solar cell applications.[288] Attempts were also made to design organosols of Os NPs and β-MnO_2 NPs using DNA as scaffolds *via* homogenous reduction route with their promising applications in catalytic hydrogenation and oxidative polymerization of pyrrole, respectively.[289,290] DNA was also been used as scaffolds to grow self assembled $NiWO_4$, $ZnWO_4$ and $MnWO_4$ nanoparticles with different

morphologies.[291–293] Fast, electroless, UV-irradiation-/microwave-assisted methods with DNA as educing as well capping agent was also been reported to synthesize continuous, electrically conductive nanowires of Au, Pd and CdS which can be used as the building blocks for functional nanodevices, miniaturized computers, sensors and optoelectronic applications.[36,294–297] Table 5 compiled self-assembled nanoclusters of versatile nanoparticles synthesized by using DNA as biotemplate or scaffold.

Likewise, owing to the presence of ultra-fine pores in their structure, biological membranes were also utilized as templates to design NPs. Rubber membrane made from the *Hevea brasiliensis* trees was used as a preservative in the production of Au NPs synthesized at the surface of membranes through the reduction of Au(III) in a solution at 80 °C for various reaction times.[301] Alternatively, a uniform size and morphology of NPs could be obtained by the use of viruses as they contain hollow spaces in the center that can be used as the template for production of particles.[302] Diatoms such as *Amphora-46* was also reported to synthesize polycrystalline Ag NPs of size ranging 20 to 25 nm under the exposure to light. This process is done by the utilization of its extract and silver nitrate ($AgNO_3$), in which the presence of a pigment known as fucoxanthin reduces the Ag ion that leads to further production of Ag NPs.[303]

2.3.3 Plant extracts for nanoparticles synthesis. Biosynthesis of NPs using plant extracts or plant biomass is one of the very effective, rapid, clean, non-toxic and eco-friendly methods. This method has been utilized predominantly to synthesize NPs of noble metals, metal oxides, bi-metallic alloys, *etc.*[304] Yun *et al.* have adequately demarcated various plant biometabolites that could help in the preparation of NPs based on their valuable role as reducing agents and capping agents. The mechanism for the phytosynthesis of metal NPs is given in Fig. 15.[305]

Kinetics of phytosynthesis of NPs is comparatively much higher to that of other biosynthesis methods and sometime equivalent to the rate of chemical routes. Shankar *et al.* reported the preparation of gold nanotriangles by treating the lemongrass leaf extract with the aqueous $AuCl^-$ ions.[306] Similarly the leaf extract of different plants like *Tamarindus indica*, *Aloe vera*, *Emblica officinalis*, *etc.* were reported to be useful for designing Au NPs.[307–309] Few-nanometer sized Pd NPs and Pt NPs were prepared using the extract taken out from various parts of different plants.[310,311] Shankar *et al.* also reported highly concentrated Ag NPs obtained from the leaf extract of *Azadirachta indica* and from the fruit extract of *Emblica officinalis*.[309,312] Li *et al.* and Leela *et al.* used the leaf extract of *Aloe vera*, *Capsicum annuum* and *Helianthus annuus* for the efficient synthesis of Ag NPs.[313,314] Extracellular production of Cu NPs was carried out using stem latex of *Euphorbia nivulia* (medicinal plant) which were found to be stabilized by the peptides and terpenoids present within the latex.[315] In a very interesting report, Seraphin *et al.* demonstrated the synthesis of In_2O_3 NPs (5–50 nm) using plant extract from *Aloe vera*.[316] Furthermore, Hou *et al.*, synthesized wurtzite ZnO NPs from Zn-hyperaccumulator plant *Sedum alfredii* with mean size of 53.7 nm.[317] Ascencio *et al.* reported the bio-assisted synthesis of iron-oxide NPs by using the biomass of *Medicago sativa* (alfalfa) plant.[318] Glutathione, an antioxidant tripeptide in plants, animals, fungi and archaea, was reported to design well-ordered aggregates of Au NPs by favouring the inter-particle interactions.[319] Kundu and Nithiyanantham also demonstrated the *in situ* fabrication of shape-selective silver nanostructures using curcumin as stabilizing and reducing agent.[320]

2.4 Key applications of different nanoparticles

NPs have wide range of applications from electronic, optoelectronic, magnetic, data storage, energy and energy storage, nanomedicines, bioimaging, *etc.* We compiled the key applications of commonly used NPs in Table 6.

3 Conclusions and future prospects

Since the inception of NPs over half a century ago, scientists are continuously exploring advanced novel methods of synthesizing NPs with the optimal size and morphology that would be beneficial for various disciplines. To engineer and fabricate an ideal size and morphology of NPs, depending upon their application/use, diverse range of physical, chemical or biological methods are already available. In this review, we provided a comprehensive overview of the commonly employed/explored strategies for the synthesis of NPs in term of their working principle, NPs designing stratagem and relevant literature. It is anticipated that this review will act as a guide article for the researchers to selectively choose particular synthesis strategy for designing the desired NPs with particular material type, size, surface properties, targeted application, *etc.*

Owing to its enormous technological potential, nanoparticles research is at the forefront. Being a leading nanomaterial in targeted drug delivery and nanomedicines, precise size with specified surface characteristics are the key desirables during nanoparticle synthesis. Cell toxicity, potential target, drug release profile, cost-effectiveness, *etc.* are the key concerns which are needed to be taken care of by the optimization of size and surface properties of nanocarriers by selecting appropriate synthesis methods. Electrospraying is growing enormously as a dry technique to design polymeric nanoparticles without using any hazardous chemicals. It provides prospects to develop nanoformulations incorporating drugs/growth factors/biomolecules with versatile structural designs like core–shell NPs, hybrid NPs, composite NPs, *etc.*, that will be useful in drug delivery, tissue engineering, biosensors, *etc.* Furthermore, electrospraying is still almost unexplored for the production of metal and ceramic nanoparticles. Plasmonics, optoelectronics, information and data storage, *etc.* are also the key areas where the synthesis strategies for the scalable production of nanoparticles needs to be further explored and optimized which can help to develop economically viable technologies.

Acknowledgements

We acknowledge the financial support received from Singapore National Research Foundation under its Translational and Clinical Research Flagship Programme (NMRC/TCR/008-SERI/

2013) and administered by the Singapore Ministry of Health's National Medical Research Council." RL thanks the SingHealth Foundation Transition Project (SHF/FG508P/2012). CD thanks the funding support from SingHealth Foundation Research Grant (SHF/FG637S/2014). NKV acknowledges Nanyang Technological University and Ministry of Education, Singapore for funding support (Grant # L0412130.010, L0412290.010 and L0421050.010).

References

1 R. P. Feynman, *Eng. Sci.*, 1960, **23**, 22–36.
2 J. Ramsden, *Essentials of Nanotechnology*, Ventus Publishing ApS, Denmark, 2009.
3 J. Lee, S. Mahendra and P. J. J. Alvarez, *ACS Nano*, 2010, **4**, 3580–3590.
4 D. M. Smith, J. K. Simon and J. R. Baker Jr, *Nat. Rev. Immunol.*, 2013, **13**, 592–606.
5 S. Nie, Y. Xing, G. J. Kim and J. W. Simons, *Annu. Rev. Biomed. Eng.*, 2007, **9**, 257–288.
6 Y. Sun, B. T. Mayers and Y. Xia, *Nano Lett.*, 2002, **2**, 481–485.
7 S. E. Skrabalak, J. Chen, Y. Sun, X. Lu, L. Au, C. M. Cobley and Y. Xia, *Acc. Chem. Res.*, 2008, **41**, 1587–1595.
8 Y. Xia, W. Li, C. M. Cobley, J. Chen, X. Xia, Q. Zhang, M. Yang, E. C. Cho and P. K. Brown, *Acc. Chem. Res.*, 2011, **44**, 914–924.
9 C. Suryanarayana and C. C. Koch, *Hyperfine Interact.*, 2000, **130**, 5–44.
10 C. B. Murray, S. Sun, W. Gaschler, H. Doyle, T. A. Betley and C. R. Kagan, *IBM J. Res. Dev.*, 2001, **45**, 47–56.
11 X. Wang, J. Zhuang, Q. Peng and Y. Li, *Nature*, 2005, **437**, 121–124.
12 J. Park, J. Joo, S. G. Kwon, Y. Jang and T. Hyeon, *Angew. Chem., Int. Ed.*, 2007, **46**, 4630–4660.
13 T. Zhu, S. G. Cloutier, I. Ivanov, K. L. Knappenberger Jr, I. Robel and F. Zhang, *J. Nanomater.*, 2012, **2012**, 1–2.
14 M. G. Panthani and B. A. Korgel, *Annu. Rev. Chem. Biomol. Eng.*, 2012, **3**, 287–311.
15 Z. W. Pan, Z. R. Dai and Z. L. Wang, *Science*, 2001, **291**, 1946–1949.
16 C. Hu, H. Liu, W. Dong, Y. Zhang, G. Bao, C. Lao and Z. L. Wang, *Adv. Mater.*, 2007, **19**, 470–474.
17 X. Wang, J. Song and Z. L. Wang, *J. Mater. Chem.*, 2007, **17**, 711–720.
18 D. Li and Y. Xia, *Adv. Mater.*, 2004, **16**, 1151–1170.
19 W. E. Teo and S. Ramakrishna, *Nanotechnology*, 2006, **17**, R89.
20 A. S. Tayi, E. T. Pashuck, C. J. Newcomb, M. T. McClendon and S. I. Stupp, *Biomacromolecules*, 2014, **15**, 1323–1327.
21 W. E. Teo and S. Ramakrishna, *Nanotechnology*, 2006, **17**, 89–106.
22 R. Vasita and D. S. Katti, *Int. J. Nanomed.*, 2006, **1**, 15–30.
23 C. J. Ellison, A. Phatak, D. W. Giles, C. W. Macosko and F. S. Bates, *Polym. J.*, 2007, **48**, 3306–3316.
24 V. Leung and F. Ko, *Polym. Adv. Technol.*, 2011, **22**, 350–365.
25 V. Beachley and X. Wen, *Mater. Sci. Eng., C*, 2009, **29**, 663–668.
26 Q. Wei, *Functional Nanofibers and their Applications*, Woodhead Publishing Limited, Cambridge, 2012; X. Luo, A. Morrin, A. J. Killard and M. R. Smyth, *Electroanalysis*, 2006, **4**, 319–326.
27 X. Luo, A. Morrin, A. J. Killard and M. R. Smyth, *Electroanalysis*, 2006, **4**, 319–326.
28 I. J. Joye and D. J. McClements, *Curr. Opin. Colloid Interface Sci.*, 2014, **19**, 1–11.
29 R. H. Baughman, A. A. Zakhidov and W. A. de Heer, *Science*, 2002, **297**, 787–792.
30 C. Zhang, Y. Yan, Y. S. Zhao and J. Yao, *Annu. Rep. Prog. Chem., Sect. C: Phys. Chem.*, 2013, **109**, 211–239.
31 H. Dai, *Acc. Chem. Res.*, 2002, **35**, 1035–1044.
32 C. Dhand, P. R. Solanki, K. N. Sood, M. Datta and B. D. Malhotra, *Electrochem. Commun.*, 2009, **11**, 1482–1486.
33 M. F. L. de Volder, S. H. Tawfick, R. H. Baughman and A. John Hart, *Science*, 2013, **339**, 535–539.
34 H. He, L. A. Pham-Huy, P. Dramou, D. Xiao, P. Zuo and C. Pham-Huy, *Int. J. Biomed. Res.*, 2013, **2013**, 1–12.
35 V. Schmidt, J. V. Wittemann, S. Senz and U. Gosele, *Adv. Mater.*, 2009, **21**, 2681–2702.
36 S. Kundu and H. Liang, *Adv. Mater.*, 2008, **20**, 826–831.
37 Y. Li, F. Qian, J. Xiang and C. M. Lieber, *Mater. Today*, 2006, **9**, 18–27.
38 J. K. Hyun, S. Zhang and L. J. Lauhon, *Annu. Rev. Mater. Res.*, 2013, **43**, 451–479.
39 M. K. Sheela Modani and M. Nijhawan, *Int. J. Curr. Pharm. Res.*, 2013, **5**, 55–59.
40 S. M. Farkhani and A. Valizadeh, *IET Nanobiotechnol.*, 2014, **8**, 59–76.
41 N. Z. Frederik Hetsch, S. V. Kershaw and A. L. Rogach, *Mater. Today*, 2013, **16**, 312–325.
42 T. Jamiesona, R. Bakhshi, D. Petrova, M. Imani and A. M. Seifalian, *Biomaterials*, 2007, **28**, 4717–4732.
43 H. Dhyani, C. Dhand, B. D. Malhotra and P. Sen, *J. Biosens. Bioelectron.*, 2011, **3**, 112.
44 H. Fischer, *Mater. Sci. Eng., C*, 2003, **23**, 763–772.
45 C. Dhand, S. K. Arya, S. P. Singh, B. P. Singh, M. Datta and B. D. Malhotra, *Carbon*, 2008, **46**, 1727–1735.
46 P. H. C. Camargo, K. G. Satyanarayana and F. Wypych, *Mater. Res.*, 2009, **12**, 1–39.
47 P. Thoniyot, M. J. Tan, A. A. Karim, D. J. Young and X. J. Loh, *Adv. Sci.*, 2015, **2**, 1400010.
48 E. Ye and X. J. Loh, *Aust. J. Chem.*, 2013, **66**, 997–1007.
49 W. H. de Jong and P. J. Borm, *Int. J. Nanomed.*, 2008, **3**, 133–149.
50 M. L. Hans and A. M. Lowman, *Curr. Opin. Solid State Mater. Sci.*, 2002, **M6**, 319–327.
51 S. Zeng, K. Yong, I. Roy, X. Dinh, X. Yu and F. Luan, *Plasmonics*, 2011, **6**, 491–506.
52 A. M. Coto-García, E. Sotelo-González, M. T. Fernández-Argüelles, R. Pereiro, J. M. Costa-Fernández and A. Sanz-Medel, *Anal. Bioanal. Chem.*, 2011, **399**, 29–42.
53 O. V. Salata, *J. Nanobiotechnol.*, 2004, **2**, 1–6.
54 M. Das, N. Saxena and P. D. Dwivedi, *Nanotoxicology*, 2009, **3**, 10–18.

55 A. Becheri, M. Durr, P. L. Nostro and P. Baglioni, *J. Nanopart. Res.*, 2008, **10**, 679–689.
56 S. Taheri, A. Cavallaro, S. N. Christo, L. E. Smith, P. Majewski, M. Barton, J. D. Hayball and K. Vasilev, *Biomaterials*, 2014, **35**, 4601–4609.
57 O. N. Gadomskii and Y. Y. Kharitonov, *Quantum Electron.*, 2004, **34**, 249–254.
58 G. E. Rachkovskaya, G. B. Zakharevich, K. V. Yumashev, A. M. Malyarevich and M. S. Gaponenko, *Glass Ceram.*, 2004, **61**, 9–10.
59 B. V. N. Nagavarma, H. K. S. Yadav, A. Ayaz, L. S. Vasudha and H. G. Shivakumar, *Asian J. Pharm. Clin. Res.*, 2012, **5**, 16–23.
60 M. Abhilash, *Int. J. Pharma Bio Sci.*, 2010, 1–12.
61 Synthesis and Patterning Methods for Nanostructures Useful for Biological Applications, in *Nanotechnology for Biology and Medicine*, ed. C. Daraio, S. Jin, G. A. Silva and V. Parpura, Springer, New York, 2012, pp. 27–44.
62 T. Xing, J. Sunarso, W. Yang, Y. Yin, A. M. Glushenkov, L. H. Li, P. C. Howlett and Y. Chen, *Nanoscale*, 2013, **5**, 7970–7976.
63 J. F. de Carvalho, S. N. de Medeiros, M. A. Morales, A. L. Dantas and A. S. Carrico, *Appl. Surf. Sci.*, 2013, **275**, 84–87.
64 S. Kar, S. Logad, O. P. Choudhary, C. Debnath, S. Verma and K. S. Bartwal, *Univers. J. Mater. Sci.*, 2013, **1**, 18–24.
65 N. Salah, S. S. Habib, Z. H. Khan, A. Memic, A. Azam, E. Alarfaj, N. Zahed and S. Al-Hamedi, *Int. J. Nanomed.*, 2011, **6**, 863–869.
66 D. Chen, X. Yi, Z. Chen, Y. Zhang and B. Chen, *Int. J. Appl. Ceram. Technol.*, 2014, **11**, 954–959.
67 M. Ullah, M. E. Ali and S. B. A. Hamid, *Rev. Adv. Mater. Sci.*, 2014, **37**, 1–14.
68 L. Zheng, B. Cui, L. Zhao, W. Li and G. C. Hadjipanayis, *J. Alloys Compd.*, 2012, **539**, 69–73.
69 K. N. Islam, A. B. Z. Zuki, M. E. Ali, M. Z. B. Hussein, M. M. Noordin, M. Y. Loqman, H. Wahid, M. A. Hakim and S. B. A. Hamid, *J. Nanomater.*, 2012, **2012**, 1–5.
70 C. Chen, Y. Chen and W. J. Tseng, *J. Mater. Process. Technol.*, 2007, **190**, 61–64.
71 M. B. Ward, R. Brydson and R. F. Cochrane, *J. Phys.: Conf. Ser.*, 2006, **26**, 296–299.
72 E. Perez-Tijerina, S. Mejia-Rosales, H. Inada and M. Jose-Yacaman, *J. Phys. Chem. C*, 2010, **114**, 6999–7003.
73 M. Maicu, R. Schmittgens, D. Hecker, D. Glob, P. Frach and G. Gerlach, *J. Vac. Sci. Technol., A*, 2014, **32**, 02B113.
74 M. Raffi, A. K. Rumaiz and M. M. Hasan, *J. Mater. Res.*, 2007, **22**, 3378–3384.
75 M. G. Pinilla, E. Martinez, G. S. Vidaurri and E. Perez-Tijerina, *Nanoscale Res. Lett.*, 2010, **5**, 180–188.
76 M. Benelmekki, J. Vernieres, J. Kim and R. Diaz, *Mater. Chem. Phys.*, 2015, **151**, 275–281.
77 K. Okuyama and I. W. Lenggoro, *Chem. Eng. Sci.*, 2003, **58**, 537–547.
78 Y. Hatakeyama, K. Onishi and K. Nishikawa, *RSC Adv.*, 2011, **1**, 1815–1821.
79 G. M. Veith, A. R. Lupini, S. J. Pennycook, A. Villa, L. Prati and N. J. Dudney, *Catal. Today*, 2007, **122**, 248–253.
80 V. Bouchat, N. Moreau, J. F. Colomer and S. Lucas, *J. Surf. Eng. Mater. Adv. Technol.*, 2013, **3**, 184–189.
81 P. Asanithi, S. Chaiyakun and P. Limsuwan, *J. Nanomater.*, 2012, **2012**, 963609.
82 D. Ichida, G. Uchida, H. Seo, K. Kamataki, N. Itagaki, K. Koga and M. Shiratani, *J. Phys.: Conf. Ser.*, 2014, **518**, 012002.
83 P. K. Ghosh, S. F. Ahmed, S. Jana and K. K. Chattopadhyay, *Opt. Mater.*, 2007, **29**, 1584–1590.
84 G. M. Veith, A. R. Lupini, S. J. Pennycook, G. W. Ownby and N. J. Dudney, *J. Catal.*, 2005, **231**, 151–158.
85 B. Ramalingam, S. Mukherjee, C. J. Mathai, K. Gangopadhyay and S. Gangopadhyay, *Nanotechnology*, 2013, **24**, 205602.
86 Y. Zhang, J. Wan, V. Skumryev, S. Stoyanov, Y. Huang, G. C. Hadjipanayis and D. Weller, *Appl. Phys. Lett.*, 2004, **85**, 5343–5345.
87 Y. K. Takahashi, T. Koyama, M. Ohnuma, T. Ohkubo and K. Hono, *J. Appl. Phys.*, 2004, **95**, 2690–2696.
88 O. Dmitrieva, M. Acet, G. Dumpich, J. Kastner, C. Antoniak, M. Farle and K. Fauth, *J. Phys. D: Appl. Phys.*, 2006, **39**, 4741–4745.
89 F. Stellacci, C. A. Bauer, T. Meyer-Friedrichsen, W. Wenseleers, V. Alain, S. M. Kuebler, S. J. K. Pond, Y. Zhang, S. R. Marder and J. W. Perry, *Adv. Mater.*, 2002, **14**, 175–198.
90 T. Hsieh, C. Chuang, Y. Chou and C. Shu, *Mater. Des.*, 2010, **31**, 1684–1687.
91 S. Uhm, D. Song, J. Kwon, S. Lee, J. Han, K. Kim and K. Kim, *Surf. Coat. Technol.*, 2013, **228**, 360–366.
92 L. Castaldi, K. Giannakopoulosa, A. Travlosa, D. Niarchosa, S. Boukarib and E. Beaurepaire, *J. Magn. Magn. Mater.*, 2005, **290–291**, 544–546.
93 A. Bello, M. Fabiane, D. Dodoo-Arhin, K. I. Ozoemena and N. Manyala, *J. Phys. Chem. Solids*, 2014, **75**, 109–114.
94 Y. Chen and C. Yeh, *Colloids Surf., A*, 2002, **197**, 133–139.
95 K. Naessens, P. van Daele and R. Baets, *SPIE-Int. Soc. Opt. Eng., Proc.*, 2001, **4426**, 124–127.
96 S. C. Singh and R. Gopal, *Bull. Mater. Sci.*, 2007, **30**, 291–293.
97 Happy, R. S. Rawat, R. V. Ramanujan, P. Lee, A. Patran, T. L. Tan, S. V. Springham and S. Lee, *31st EPS Conference on Plasma Phys.*, London, 2004, vol. 28G, pp. 1–4.
98 P. L. Ong, S. Mahmood, T. Zhang, J. J. Lin, R. V. Ramanujan, P. Lee and R. S. Rawat, *Appl. Surf. Sci.*, 2008, **254**, 1909–1914.
99 C. D. Andrea, F. Neri, P. M. Ossi, N. Santo and S. Trusso, *Nanotechnology*, 2009, **20**, 245606.
100 Y. Jing, H. Wang, X. Chen, X. Wang, H. Wei and Z. Guo, *Appl. Surf. Sci.*, 2014, **316**, 66–71.
101 D. Kumar, S. Yarmolenko, J. Sankar, J. Narayan, H. Zhou and A. Tiwari, *Composites, Part B*, 2004, **35**, 149–155.
102 M. Quintana, E. Haro-Poniatowski, J. Morales and N. Batina, *Appl. Surf. Sci.*, 2002, **195**, 175–186.
103 J. J. Lin, L. S. Loh, P. Lee, T. L. Tan, S. V. Springham and R. S. Rawat, *Appl. Surf. Sci.*, 2009, **255**, 4372–4377.

104 S. Amoruso, G. Ausanio, C. de Lisio, V. Iannotti, M. Vitiello, X. Wang and L. Lanotte, *Appl. Surf. Sci.*, 2005, **247**, 71–75.
105 M. S. Dhlamini, J. J. Terblans, O. M. Ntwaeaborwa, J. M. Ngaruiya, K. T. Hillie, J. R. Botha and H. C. Swart, *J. Lumin.*, 2008, **128**, 1997–2003.
106 M. K. Akbari, R. Derakhshan and O. Mirzaee, *Chem. Eng. J.*, 2015, **259**, 918–926.
107 J. P. Lei, X. L. Dong, X. G. Zhu, M. K. Lei, H. Huang, X. F. Zhang, B. Lu, W. J. Park and H. S. Chung, *Intermetallics*, 2007, **15**, 1589–1594.
108 G. A. J. Amaratunga, M. Chhowalla, C. J. Kiely, I. Alexandrou, R. Aharonov and R. M. Devenish, *Nature*, 1996, **383**, 321–323.
109 M. Chhowalla and G. A. J. Amaratunga, *Nature*, 2000, **407**, 164–167.
110 R. D. Amato, M. Falconieri, S. Gagliardi, E. Popovici, E. Serra, G. Terranova and E. Borsella, *J. Anal. Appl. Pyrolysis*, 2013, **104**, 461–469.
111 M. Scarisoreanu, R. Alexandrescu, I. Morjan, R. Birjega, C. Luculescu, E. Popovici, E. Dutu, E. Vasile, V. Danciu and N. Herlin-Boime, *Appl. Surf. Sci.*, 2013, **278**, 295–300.
112 E. Marino, B. Bouchet-Fabre, D. Porterat and C. Reynaud, *Diamond Relat. Mater.*, 2005, **14**, 1120–1125.
113 I. Llamas-Jansa, C. Jager, H. Mutschke and T. Henning, *Carbon*, 2007, **45**, 1542–1557.
114 M. T. Swihart, *Curr. Opin. Colloid Interface Sci.*, 2003, **8**, 127–133.
115 S. Veintemillas-Verdaguer, Y. Leconte, R. Costo, O. Bomati-Miguel, B. Bouchet-Fabre, M. P. Morales, P. Bonville, S. Perez-Rial, I. Rodriguez and N. Herlin-Boime, *J. Magn. Magn. Mater.*, 2007, **311**, 120–124.
116 O. Bomatí-Miguel, P. Tartaj, M. P. Morales, P. Bonville, U. Golla-Schindler, X. Q. Zhao and S. Veintemillas-Verdaguer, *Small*, 2006, **2**, 1476–1483.
117 F. Erogbogbo, K. Yong, I. Roy, G. X. Xu, P. N. Prasad and M. T. Swihart, *ACS Nano*, 2008, **2**, 873–878.
118 W. Y. Teoh, R. Amal and L. Madler, *Nanoscale*, 2010, **2**, 1324–1347.
119 M. Sokolowski, A. Sokolowska, A. Michalski and B. Gokieli, *J. Aerosol Sci.*, 1977, **8**, 219–230.
120 T. R. Hinklin, S. C. Rand and R. M. Laine, *Adv. Mater.*, 2008, **20**, 1270–1273.
121 T. Sahma, L. Madler, A. Gurlo, N. Barsan, S. E. Pratsinis and U. Weimar, *Sens. Actuators, B*, 2004, **98**, 148–153.
122 H. Schulz, L. Mädler, S. E. Pratsinis, P. Burtscher and N. Moszner, *Adv. Funct. Mater.*, 2005, **15**, 830–837.
123 R. N. Grass, E. K. Athanassiou and W. J. Stark, *Angew. Chem., Int. Ed.*, 2007, **46**, 4909–4912.
124 O. Arutanti, A. B. D. Nandiyanto, T. Ogi, F. Iskandar, T. O. Kim and K. Okuyama, *J. Alloys Compd.*, 2014, **591**, 121–126.
125 D. Channei, B. Inceesungvorn, N. Wetchakun, S. Phanichphant, A. Nakaruk, P. Koshy and C. C. Sorrell, *Ceram. Int.*, 2013, **39**, 3129–3134.
126 C. Siriwong, N. Tamaekong and S. Phanichphant, *Mater. Lett.*, 2012, **68**, 97–100.
127 J. A. Bhushani and C. Anandharamakrishnan, *Trends Food Sci. Technol.*, 2014, **38**, 21–33.
128 R. Sridhar, R. Lakshminarayanan, K. Madhaiyan, V. A. Barathi, K. H. C. Lim and S. Ramakrishna, *Chem. Soc. Rev.*, 2015, **44**, 790–814.
129 P. H. M. Bottger, Z. Bi, D. Adolph, K. A. Dick, L. S. Karlsson, M. N. A. Karlsson, B. A. Wacaser and K. Deppert, *Nanotechnology*, 2007, **18**, 1–6.
130 R. Sridhar and S. Ramakrishna, *Biomatter*, 2013, **3**, e24281.
131 M. Zamani, M. P. Prabhakaran, E. S. Thian and S. Ramakrishna, *Int. J. Pharm.*, 2014, **473**, 134–143.
132 G. Pyrgiotakis, J. McDevitt, A. Bordini, E. Diaz, R. Molina, C. Watson, G. Deloid, S. Lenard, N. Fix, Y. Mizuyama, T. Yamauchi, J. Brain and P. Demokritou, *Environ. Sci.: Nano*, 2014, **1**, 15–26.
133 A. Jaworek, A. T. Sobczyk, A. Krupa, M. Lackowski and T. Czech, *Bull. Pol. Acad. Sci.: Tech. Sci.*, 2009, **57**, 63–70.
134 W. Cai, T. Gao, H. Hong and J. Sun, *Nanotechnol., Sci. Appl.*, 2008, **1**, 17–32.
135 M. Valvo, U. Lafont and D. Munao, *J. Power Sources*, 2009, **189**, 297–302.
136 S. Prabhu and E. K. Poulose, *Int. Nano Lett.*, 2012, **2**, 1–10.
137 T. Krishnakumar, R. Jayaprakash, V. N. Singh, B. R. Mehta and A. R. Phani, *J. Nano Res.*, 2008, **4**, 91–101.
138 S. S. Chee and J. H. Lee, *Trans. Nonferrous Met. Soc. China*, 2012, **22**, 707–711.
139 A. Jaworek and A. T. Sobczyk, *J. Electrost.*, 2008, **66**, 197–219.
140 L. Tang and J. Cheng, *Nano Today*, 2013, **8**, 290–312.
141 S. M. Haidary, E. P. Corcoles and N. K. Ali, *J. Nanomater.*, 2012, **2012**, 15.
142 S. Witharana, C. Hodges, D. Xu, X. Lai and Y. Ding, *J. Nanopart. Res.*, 2012, **14**, 1–11.
143 F. Alonso, P. Riente, J. A. Sirvent and M. Yus, *Appl. Catal., A*, 2010, **378**, 42–51.
144 H. Shi, R. Magaye, V. Castranova and J. Zhao, *Part. Fibre Toxicol.*, 2013, **10**, 1–33.
145 M. Eshed, S. Pol, A. Gedanken and M. Balasubramanian, *Beilstein J. Nanotechnol.*, 2011, **2**, 198–203.
146 S. A. Jamal, *Chem. Sci. J.*, 2013, **2013**, 1–10.
147 J. V. Erven, R. Moerman and J. C. M. Marijnissen, *Aerosol Sci. Technol.*, 2005, **39**, 941–946.
148 S. S. Nkosi, B. W. Mwakikunga, E. Sideras-Haddad and A. Forbes, *Nanotechnol., Sci. Appl.*, 2012, **5**, 27–36.
149 M. R. Diaz and P. E. Vivas-Mejia, *Pharmaceuticals*, 2013, **6**, 1361–1380.
150 L. Y. Yeo, Z. Gagnon and H. C. Chang, *Biomaterials*, 2005, **26**, 6122–6128.
151 L. Cismaru and M. Popa, *Rev. Roum. Chim.*, 2010, **55**, 433–442.
152 C. J. Luo, T. Okubo, M. Nangrejob and M. Edirisinghe, *Polym. Int.*, 2015, **64**, 183–187.
153 K. Matsukawa, M. Watanabe, T. Hamada, T. Nagase and H. Naito, *Int. J. Polym. Sci.*, 2012, **2012**, 10.
154 E. C. Cho, Y. K. Hwang and U. Jeong, *Bull. Korean Chem. Soc.*, 2014, **35**, 1784–1788.
155 L. Buruaga and J. A. Pomposo, *Polymers*, 2011, **3**, 1673–1683.

156 Y. Wu and R. L. Clark, *J. Biomater. Sci., Polym. Ed.*, 2008, **9**, 573–601.
157 N. Dubey, R. Varshney, J. Shukla, A. Ganeshpurkar, P. P. Hazari, G. P. Bandopadhaya, A. K. Mishra and P. Trivedi, *Drug Delivery*, 2012, **19**, 132–142.
158 Y. Ma, Y. Zheng, X. Zeng, L. Jiang, H. Chen, R. Liu, L. Huang and L. Mei, *Int. J. Nanomed.*, 2011, **6**, 2679–2688.
159 U. Nagarajan, K. Kawakami, S. Zhang, B. Chandrasekaran and B. U. Nair, *Chem. Pharm. Bull.*, 2014, **62**, 422–428.
160 M. Papi, V. Palmieri, G. Maulucci, G. Arcovito, E. Greco, G. Quintiliani, M. Fraziano and M. de Spirito, *J. Nanopart. Res.*, 2011, **13**, 6141–6147.
161 L. Peltonen, H. Valo, R. Kolakovic, T. Laaksonen and J. Hirvonen, *Expert Opin. Drug Delivery*, 2010, **7**, 705–719.
162 S. K. Nitta and K. Numata, *Int. J. Mol. Sci.*, 2013, **14**, 1629–1654.
163 N. Karak, *Fundamentals Of Polymers: Raw Materials To Finish Products*, Prentice-hall Of India Pvt Ltd, New Delhi, 1st edn, 2009.
164 B. Lin, U. Sundararaj and P. Potschke, *Macromol. Mater. Eng.*, 2006, **291**, 227–238.
165 B. Sevil and K. Zuhal, *Macromol. Symp.*, 2010, **295**, 59–64.
166 H. S. Lee, L. Zhu and R. A. Weiss, *Polymer*, 2005, **46**, 10841–10853.
167 *Sol-Gel Science: The Physics and Chemistry of Sol-Gel Processing*, ed. C. J. Brinker and G. W. Scherer, Academic Press, USA, 1990, e-book, http://depts.washington.edu/solgel/documents/class_docs/MSE502/SolGel_Science_The_physics_and_chemistry_of_sol-gel_processing_-_Brinker_1990.pdf.
168 M. A. Behnajady, H. Eskandarloo, N. Modirshahla and M. Shokri, *Desalination*, 2011, **278**, 10–17.
169 M. Aziz, S. S. Abbas and W. R. W. Baharom, *Mater. Lett.*, 2013, **91**, 31–34.
170 L. F. F. F. Goncalves, F. K. Kanodarwala, J. A. Stride, C. J. R. Silva, M. R. Pereira and M. J. M. Gomes, *J. Photochem. Photobiol., A*, 2014, **285**, 21–29.
171 N. Bayal and P. Jeevanandam, *J. Alloys Compd.*, 2012, **516**, 27–32.
172 P. Nautiyal, M. M. Seikh, O. I. Lebedev and A. K. Kundu, *J. Magn. Magn. Mater.*, 2015, **377**, 402–405.
173 S. M. Reda, *Mater. Sci. Semicond. Process.*, 2010, **13**, 417–425.
174 Y. Zhang, R. Li, Y. Jiang, B. Zhao, H. Duan, J. Li and Z. Feng, *J. Solid State Chem.*, 2011, **184**, 2047–2052.
175 N. Chumha, S. Kittiwachana, T. Thongtem, S. Thongtem and S. Kaowphong, *Mater. Lett.*, 2014, **136**, 18–21.
176 T. Sreethawong, S. Ngamsinlapasathian and S. Yoshikawa, *J. Mol. Catal. A: Chem.*, 2013, **374–375**, 94–101.
177 J. N. Solanki and Z. V. P. Murthy, *Ind. Eng. Chem. Res.*, 2011, **50**, 12311–12323.
178 M. A. Malik, M. Y. Wani and M. A. Hashim, *Arabian J. Chem.*, 2012, **5**, 397–417.
179 M. Boutonnet, J. Kizling and P. Stenius, *Colloids Surf.*, 1982, **5**, 209–225.
180 R. A. Martınez-Rodriguez, F. J. Vidal-Iglesias, J. Solla-Gullon, C. R. Cabrera and J. M. Feliu, *J. Am. Chem. Soc.*, 2014, **136**, 1280–1283.
181 W. Zhang, X. Qia, J. Chen and H. Wang, *J. Colloid Interface Sci.*, 2006, **302**, 370–373.
182 W. Zhang, X. Qia and J. Chen, *J. Chem. Phys.*, 2006, **330**, 495–500.
183 M. P. Pileni and I. Lisiecki, *Colloids Surf., A*, 1993, **80**, 63–68.
184 C. Petit, P. Lixon and M. P. Pileni, *J. Phys. Chem.*, 1990, **94**, 1598–1603.
185 D. H. Chen and S. H. Wu, *Chem. Mater.*, 2000, **12**, 1354–1360.
186 S. Kundu, *J. Mater. Chem. C*, 2013, **1**, 831–842.
187 S. Kundu, K. Wang and H. Liang, *J. Phys. Chem. C*, 2009, **113**, 18570–18577.
188 S. Praharaj, S. K. Ghosh, S. Nath, S. Kundu, S. Panigrahi, S. Basu and T. Pal, *J. Phys. Chem. B*, 2005, **109**, 13166–13174.
189 S. Y. Chang, L. Liu and S. A. Asher, *J. Am. Chem. Soc.*, 1994, **116**, 6739–6744.
190 D. H. Chen and C. J. Chen, *J. Mater. Chem.*, 2002, **12**, 1557–1562.
191 S. Vaucher, J. Fielden, M. Li, E. Dujardin and S. Mann, *Nano Lett.*, 2002, **2**, 225–229.
192 M. Mandal, S. Kundu, S. K. Ghosh and T. Pal, *J. Photochem. Photobiol., A*, 2004, **167**, 17–22.
193 S. S. Atik and J. K. Thomas, *J. Am. Chem. Soc.*, 1981, **103**, 4279–4280.
194 M. P. Pileni, *C. R. Chim.*, 2003, **6**, 965–978.
195 S. Holdcroft and J. E. Guillet, *J. Polym. Sci., Part A: Polym. Chem.*, 1990, **28**, 1823–1829.
196 W. R. P. Raj, M. Sasthav and H. M. Cheung, *Langmuir*, 1991, **7**, 2586–2591.
197 C. Destree and J. B. Nagy, *Adv. Colloid Interface Sci.*, 2006, **123–126**, 353–367.
198 C. Yang, Z. Junhua and W. Guanghui, *J. Wuhan Univ. Technol., Mater. Sci. Ed.*, 2013, **28**, 787–792.
199 Z. Wang, Y. Wang, D. Xu, E. S. W. Kong and Y. Zhang, *Synth. Met.*, 2010, **160**, 921–926.
200 C. Dhand, M. Das, G. Sumana, A. K. Srivastava, M. K. Pandey, C. G. Kim, M. Datta and B. D. Malhotra, *Nanoscale*, 2010, **2**, 747–754.
201 H. Hayashi and Y. Hakuta, *Materials*, 2010, **3**, 3794–3817.
202 A. Abedini, A. R. Daud, M. A. A. Hamid, N. K. Othman and E. Saion, *Nanoscale Res. Lett.*, 2013, **8**, 1–10.
203 J. J. Du, C. Chen, Y. L. Gan, R. H. Zhang, C. Y. Yang and X. W. Zhou, *Int. J. Hydrogen Energy*, 2014, **39**, 17634–17637.
204 Y. Ma, M. Chen and M. Li, *Mater. Lett.*, 2015, **139**, 22–25.
205 X. D. Liu, H. Chen, S. S. Liu, L. Q. Ye and Y. P. Li, *Mater. Res. Bull.*, 2015, **62**, 217–221.
206 M. Tadic, M. Panjan, V. Damnjanovic and I. Milosevic, *Appl. Surf. Sci.*, 2014, **320**, 183–187.
207 K. Sue, S. Kawasaki, M. Suzuki, Y. Hakuta, H. Hayashi, K. Arai, Y. Takebayashi, S. Yoda and T. Furuya, *Chem. Eng. J.*, 2011, **166**, 947–953.
208 D. Zhao, X. Wu, H. Guan and E. Han, *J. Supercrit. Fluids*, 2007, **42**, 226–233.
209 J. Yang and J. Pan, *Acta Mater.*, 2012, **60**, 4753–4758.

210 J. Guo, X. Zhou, Y. Lu, X. Zhang, S. Kuang and W. Hou, *J. Solid State Chem.*, 2012, **196**, 550–556.
211 B. H. Choi, S. Park, B. K. Park, H. H. Chun and Y. Kim, *Mater. Res. Bull.*, 2013, **48**, 3651–3656.
212 Y. Cao, P. Hu and D. Jia, *Appl. Surf. Sci.*, 2013, **265**, 771–777.
213 A. Behbahani, S. Rowshanzamir and A. Esmaeilifar, *Procedia Eng.*, 2012, **42**, 908–917.
214 E. Maryanti, D. Damayanti, I. Gustian and S. Y. Salprima, *Mater. Lett.*, 2014, **118**, 96–98.
215 P. Rahman and M. Green, *Nanoscale*, 2009, **1**, 214–224.
216 T. Herricks, J. Chen and Y. Xia, *Nano Lett.*, 2004, **2**, 2367–2371.
217 B. K. Park, S. Jeong, D. Kim, J. Moon, S. Lim and J. S. Kim, *J. Colloid Interface Sci.*, 2007, **311**, 417–424.
218 D. Kim, S. Jeong and J. Moon, *Nanotechnology*, 2006, **17**, 4019–4024.
219 M. H. Kim, B. Lim, E. P. Lee and Y. Xia, *J. Mater. Chem.*, 2008, **18**, 4069–4073.
220 R. J. Joseyphus and B. Jeyadevan, *J. Phys. Chem. Solids*, 2011, **72**, 1212–1217.
221 S. Lee, S. Jeong, D. Kim, S. Hwang, M. Jeon and J. Moon, *Superlattices Microstruct.*, 2008, **43**, 330–339.
222 M. Ahrén, L. Selegard, F. Soderlind, M. Linares, J. Kauczor, P. Norman, P. Kall and K. Uvdal, *J. Nanopart. Res.*, 2012, **14**, 1–17.
223 C. Quievryn, S. Bernard and P. Miele, *Nanomater. Nanotechnol.*, 2014, **4**, 1–8.
224 N. Songvorawit, K. Tuitemwong and P. Tuitemwong, *ISRN Nanotechnol.*, 2011, **2011**, 483129.
225 C. Cheng, F. Xu and H. Gu, *New J. Chem.*, 2011, **35**, 1072–1079.
226 K. Isogai and T. Itoh, *Proceedings of International Symposium on EcoTopia Science, ISETS07*, 2007, pp. 155–157.
227 M. Zamanpour, Y. Chen, B. Hu, K. Carroll, Z. J. Huba, E. E. Carpenter, L. H. Lewis and V. G. Harris, *J. Appl. Phys.*, 2012, **111**, 07B528.
228 M. T. Swihart, *Curr. Opin. Colloid Interface Sci.*, 2003, **8**, 127–133.
229 S. Polarz, A. Roy, M. Merz, S. Halm, D. Schroder, L. Schneider, G. Bacher, F. E. Kruis and M. Driess, *Small*, 2005, **1**, 540–552.
230 S. Hartner, M. Ali, C. Schulz, M. Winterer and H. Wiggers, *Nanotechnology*, 2009, **20**, 445701.
231 W. Jin, I. Lee, A. Kompch, U. Dorfler and M. Winterer, *J. Eur. Ceram. Soc.*, 2007, **27**, 4333–4337.
232 J. Suffner, P. Agoston, J. Kling and H. Hahn, *J. Nanopart. Res.*, 2010, **12**, 2579–2588.
233 A. Lahde, N. Kokkonen, A. J. Karttunen, S. Jaaskelainen, U. Tapper, T. A. Pakkanen and J. Jokiniemi, *J. Nanopart. Res.*, 2011, **13**, 3591–3598.
234 D. Lee, O. V. Tolochko, F. R. Turaev, D. Kim and B. Kim, *J. Nanosci. Nanotechnol.*, 2009, **9**, 1–6.
235 J. Ruusunen, M. Ihalainen, T. Koponen, T. Torvela, M. Tenho, J. Salonen, O. Sippula, J. Joutsensaari, J. Jokiniemi and A. Lahde, *J. Nanopart. Res.*, 2014, **16**, 1–11.
236 J. Lee, C. Lee and K. Lee, *IOP Conf. Ser.: Mater. Sci. Eng.*, 2011, **18**, 1–6.
237 M. Shimada, W. Wang and K. Okuyama, *Chem. Vap. Deposition*, 2010, **16**, 151–156.
238 N. Dwivedi, S. Kumar and H. K. Malik, *ACS Appl. Mater. Interfaces*, 2011, **3**, 4268–4278.
239 N. Dwivedi, S. Kumar, Ishpal, S. Dayal, Govind, C. M. S. Rauthan and O. S. Panwar, *J. Alloys Compd.*, 2011, **509**, 1285–1293.
240 N. Dwivedi, S. Kumar, R. K. Tripathy, J. D. Carey, H. K. Malik and M. K. Dalai, *ACS Appl. Mater. Interfaces*, 2012, **4**, 5309–5316.
241 N. Dwivedi, S. Kumar, J. D. Carey, R. K. Tripathy, H. K. Malik and M. K. Dalai, *ACS Appl. Mater. Interfaces*, 2013, **5**, 2725–2732.
242 N. Dwivedi, S. Kumar, H. K. Malik, C. M. S. Rauthan and O. S. Panwar, *Mater. Chem. Phys.*, 2011, **130**, 775–785.
243 N. Dwivedi, S. Kumar and H. K. Malik, *J. Appl. Phys.*, 2012, **112**, 023518.
244 N. Dwivedi, S. Kumar, R. K. Tripathy, H. K. Malik and O. S. Panwar, *Appl. Phys. A*, 2011, **105**, 417–425.
245 X. Wang, Z. Hu, X. Chen and Y. Chen, *Scr. Mater.*, 2001, **44**, 1567–1570.
246 H. Vach, Q. Brulin, N. Chaabane, T. Novikova, P. R. Cabarrocas, B. Kalache, K. Hassouni, S. Botti and L. Reining, *Comput. Mater. Sci.*, 2006, **35**, 216–222.
247 J. Yun, T. Bae, J. Kwon, S. Lee and G. Lee, *Nanoscale*, 2012, **4**, 7221.
248 Y. Zhu, S. Murali, W. Cai, X. Li, J. W. Suk, J. R. Potts and R. S. Ruoff, *Adv. Mater.*, 2010, **22**, 3906–3924.
249 W. S. Hummers and R. E. Offeman, *J. Am. Chem. Soc.*, 1958, **80**, 1339.
250 X. Zhao, L. Liu, X. Li, J. Zeng, X. Jia and P. Liu, *Langmuir*, 2014, **30**, 10419–10429.
251 B. Jana, A. Biswas, S. Mohapatra, A. Saha and S. Ghosh, *Chem. Commun.*, 2014, **50**, 11595–11598.
252 B. Jana, G. Mondal, A. Biswas, I. Chakraborty, A. Saha, P. Kurkute and S. Ghosh, *Macromol. Biosci.*, 2013, **13**, 1478–1484.
253 J. L. Li, H. C. Bao, X. L. Hou, L. Sun, X. G. Wang and M. Gu, *Angew. Chem., Int. Ed.*, 2012, **51**, 1830–1834.
254 X. Zhang, S. Yan, R. D. Tyagi and R. Y. Surampalli, *Chemosphere*, 2011, **82**, 489–494.
255 A. Nanda and M. Saravanan, *Nanomedicine*, 2009, **5**, 452–456.
256 L. Sintubin, W. D. Windt, J. Dick, J. Mast, D. V. Ha, W. Verstraete and N. Boon, *Appl. Microbiol. Biotechnol.*, 2009, **84**, 741–749.
257 K. Prasad, A. K. Jha and A. R. Kulkarni, *Nanoscale Res. Lett.*, 2007, **2**, 248–250.
258 M. M. G. Babu and P. Gunasekaran, *Colloids Surf., B*, 2009, **74**, 191–195.
259 R. Y. Sweeney, C. Mao, X. Gao, J. L. Burt, A. M. Belcher, G. Georgiou and B. L. Iverson, *Chem. Biol.*, 2004, **11**, 1553–1559.
260 N. Sharma, A. K. Pinnaka, M. Raje, A. Fnu, M. S. Bhattacharyya and A. R. Choudhury, *Microb. Cell Fact.*, 2012, **11**, 1–6.

261 P. Mukherjee, A. Ahmad, D. Mandal, S. Senapati, S. R. Sainkar, M. I. Khan, R. Parishcha, P. V. Ajaykumar, M. Alam, R. Kumar and M. Sastry, *Nano Lett.*, 2001, **1**, 515–519.
262 G. Li, D. He, Y. Qian, B. Guan, S. Gao, Y. Cui, K. i. Yokoyama and L. Wang, *Int. J. Mol. Sci.*, 2012, **13**, 466–476.
263 D. B. Raudabaugh, M. B. Tzolov, J. P. Calabrese and B. E. Overton, *Nanomater. Nanotechnol.*, 2013, **3**, 1–6.
264 N. Vigneshwaran, N. M. Ashtaputre, P. V. Varadarajan, R. P. Nachane, K. M. Paralikar and R. H. Balasubramanya, *Mater. Lett.*, 2007, **61**, 1413–1418.
265 R. Devika, S. Elumalai, E. Manikandan and D. Eswaramoorthy, *Sci. Rep.*, 2012, **1**, 1–5.
266 A. Chauhan, S. Zubair, S. Tufail, A. Sherwani, M. Sajid, S. C. Raman, A. Azam and M. Owais, *Int. J. Nanomed.*, 2011, **6**, 2305–2319.
267 M. Kitching, M. Ramani and E. Marsili, *Microb. Biotechnol.*, 2014, 1–14, DOI: 10.1111/1751-7915.12151.
268 V. Bansal, A. Ahmad and M. Sastry, *J. Am. Chem. Soc.*, 2006, **128**, 14059–14066.
269 A. Bharde, D. Rautaray, V. Bansal, A. Ahmad, I. Sarkar, S. M. Yusuf, M. Sanyal and M. Sastry, *Small*, 2006, **2**, 135–141.
270 V. Bansal, D. Rautaray, A. Bharde, K. Ahire, A. Sanyal, A. Ahmad and M. Sastry, *J. Mater. Chem.*, 2005, **15**, 2583–2589.
271 V. Bansal, D. Rautaray, A. Ahmad and M. Sastry, *J. Mater. Chem.*, 2004, **14**, 3303–3305.
272 M. Kowshik, S. Ashtaputre, S. Kharrazi, W. Vogel, J. Urban, S. K. Kulkarn and K. M. Paknikar, *Nanotechnology*, 2003, **14**, 95–100.
273 K. K. Sathish, R. Amutha, P. Arumugam and S. Berchmans, *ACS Appl. Mater. Interfaces*, 2011, **3**, 1418–1425.
274 P. S. Pimprikar, S. S. Joshi, A. R. Kumar, S. S. Zinjarde and S. K. Kulkarni, *Colloids Surf., B*, 2009, **74**, 309–316.
275 C. T. Dameron, R. N. Reese, R. K. Mehra, A. R. Kortan, P. J. Carroll, M. L. Steigerwald, L. E. Brus and D. R. Winge, *Nature*, 1989, **338**, 596–597.
276 S. Seshadri, K. Saranya and M. Kowshik, *Biotechnol. Prog.*, 2011, **27**, 1464–1469.
277 A. Ahmad, S. Senapati, M. I. Khan, R. Kumar and M. Sastry, *Langmuir*, 2003, **19**, 3550–3553.
278 E. Torres-Chavolla, R. J. Ranasinghe and E. C. Alocilja, *IEEE Trans. Nanotechnol.*, 2010, **9**, 533–538.
279 A. Bharde, A. Kulkarni, M. Rao, A. Prabhune and M. Sastry, *J. Nanosci. Nanotechnol.*, 2007, **7**, 4369–4377.
280 A. Sinha and S. K. Khare, *Bioresour. Technol.*, 2011, **102**, 4281–4284.
281 H. Bao, Z. Lu, X. Cui, Y. Qiao, J. Guo, J. M. Anderson and C. M. Li, *Acta Biomater.*, 2010, **6**, 3534–3541.
282 P. Mukherjee, S. Senapati, D. Mandal, A. Ahmad, M. I. Khan, R. Kumar and M. Sastry, *ChemBioChem*, 2002, **3**, 461–463.
283 A. Ahmad, S. Senapati, M. I. Khan, R. Kumar, R. Ramani, V. Srinivas and M. Sastry, *Nanotechnology*, 2003, **14**, 824–828.
284 A. Zinchenko, Y. Miwa, L. I. Lopatina, V. G. Sergeyev and S. Murata, *ACS Appl. Mater. Interfaces*, 2014, **6**, 3226–3232.
285 D. Majumdar, A. Singha, P. K. Mondal and S. Kundu, *ACS Appl. Mater. Interfaces*, 2013, **5**, 7798–7807.
286 S. Kundu, *Phys. Chem. Chem. Phys.*, 2013, **15**, 14107–14119.
287 S. Kundu, V. Maheshwari and R. F. Saraf, *Langmuir*, 2008, **24**, 551–555.
288 S. Kundu and U. Nithiyanantham, *Ind. Eng. Chem. Res.*, 2014, **53**, 13667–13679.
289 S. Anantharaj, U. Nithiyanantham, S. R. Ede and S. Kundu, *Ind. Eng. Chem. Res.*, 2014, **53**, 19228–19238.
290 S. R. Ede, S. Anantharaj, U. Nithiyanantham and S. Kundu, *Phys. Chem. Chem. Phys.*, 2015, **17**, 5474–5484.
291 U. Nithiyanantham, S. R. Ede, S. Anantharaj and S. Kundu, *Cryst. Growth Des.*, 2015, **15**, 673–686.
292 S. R. Ede, A. Ramadoss, U. Nithiyanantham, S. Anantharaj and S. Kundu, *Inorg. Chem.*, 2015, **54**, 3851–3863.
293 U. Nithiyanantham, S. R. Ede, T. Kesavan, P. Ragupathy, M. D. Mukadam, S. M. Yusuf and S. Kundu, *RSC Adv.*, 2014, **4**, 38169–38181.
294 S. Kundu, K. Wang, D. Huitink and H. Liang, *Langmuir*, 2009, **25**, 10146–10152.
295 S. Kundu, H. Lee and H. Liang, *Inorg. Chem.*, 2009, **48**, 121–127.
296 S. Kundu and H. Liang, *Langmuir*, 2008, **24**, 9668–9674.
297 S. Kundu and M. Jayachandran, *RSC Adv.*, 2013, **3**, 16486–16498.
298 U. Nithiyanantham, S. R. Ede and S. Kundu, *J. Mater. Chem. C*, 2014, **2**, 3782–3794.
299 S. R. Ede, A. Ramadoss, S. Anantharaj, U. Nithiyanantham and S. Kundu, *Phys. Chem. Chem. Phys.*, 2014, **16**, 21846–21859.
300 U. Nithiyanantham, A. Ramadoss, S. R. Ede and S. Kundu, *Nanoscale*, 2014, **6**, 8010–8023.
301 F. C. Cabrera, H. Mohan, R. J. D. Santos, D. L. S. Agostini, R. F. Aroca, M. A. Rodríguez-Pérez and A. E. Job, *J. Nanomater.*, 2013, **2013**, 1–10.
302 J. K. Pokorski and N. F. Steinmetz, *Mol. Pharm.*, 2011, **8**, 29–43.
303 J. Jena, N. Pradhan, B. P. Dash, P. K. Panda and B. K. Mishra, *J. Saudi Chem. Soc.*, 2014, 1–6.
304 S. Iravani, *Green Chem.*, 2011, **13**, 2638–2650.
305 M. S. Akhtar, J. Panwar and Y. Yun, *ACS Sustainable Chem. Eng.*, 2013, **1**, 591–602.
306 S. S. Shankar, A. Rai, B. Ankamwar, A. Singh, A. Ahmad and M. Sastry, *Synth. React. Inorg., Met.-Org., Nano-Met. Chem.*, 2014, **3**, 482–488.
307 S. P. Chandran, M. Chaudhary, R. Pasricha, A. Ahmad and M. Sastry, *Biotechnol. Prog.*, 2006, **22**, 577–583.
308 B. Ankamwar, M. Chaudhary and M. Sastry, *Synth. React. Inorg., Met.-Org., Nano-Met. Chem.*, 2005, **35**, 19–26.
309 B. Ankamwar, C. Damle, A. Ahmad and M. Sastry, *J. Nanosci. Nanotechnol.*, 2005, **5**, 1665–1671.
310 F. Coccia, L. Tonucci, D. Bosco, M. Bressand and N. Alessandro, *Green Chem.*, 2012, **14**, 1073–1078.
311 M. Sathishkumar, K. Sneha, I. S. Kwak, J. Mao, S. J. Tripathy and Y. S. Yun, *J. Hazard. Mater.*, 2009, **171**, 400–404.

312 S. S. Shankar, A. Rai, A. Ahmad and M. Sastry, *J. Colloid Interface Sci.*, 2004, **275**, 496–502.
313 A. Leela and M. Vivekanandan, *Afr. J. Biotechnol.*, 2008, **7**, 3162–3165.
314 S. Li, Y. Shen, A. Xie, X. Yu, L. Qiu, L. Zhang and Q. Zhang, *Green Chem.*, 2007, **9**, 852–858.
315 V. Vellora, T. Padil and M. Cernik, *Int. J. Nanomed.*, 2013, **8**, 889–898.
316 S. Maensiri, P. Laokul, J. Klinkaewnarong, S. Phokha, V. Promarak and S. Seraphin, *J. Optoelectron. Adv. Mater.*, 2008, **10**, 161–165.
317 J. Qu, C. Luo and J. Hou, *Micro Nano Lett.*, 2011, **6**, 174–176.
318 R. Herrera-Becerra, C. Zorrilla, J. L. Rius and J. A. Ascencio, *Appl. Phys. A*, 2008, **91**, 241–246.
319 S. Basu, S. K. Ghosh, S. Kundu, S. Panigrahi, S. Praharaj, S. Pande, S. Jana and T. Pal, *J. Colloid Interface Sci.*, 2007, **313**, 724–734.
320 S. Kundu and U. Nithiyanantham, *RSC Adv.*, 2013, **3**, 25278–25290.
321 M. M. Kholoud, A. El-Nour, A. Eftaiha, A. Al-Warthan and R. A. A. Ammar, *Arabian J. Chem.*, 2010, **3**, 135–140.
322 C. Rigo, L. Ferroni, I. Tocco, M. Roman, I. Munivrana, C. Gardin, W. R. L. Cairns, V. Vindigni, B. Azzena, C. Barbante and B. Zavan, *Int. J. Mol. Sci.*, 2013, **14**, 4817–4840.
323 V. Ambrogi, A. Donnadio, D. Pietrella, L. Latterini, F. A. Proietti, F. Marmottini, G. Padeletti, S. Kaciulis, S. Glovagnoli and M. Ricci, *J. Mater. Chem. B*, 2014, **2**, 6054–6063.
324 M. Jeyaraj, G. Sathishkumar, G. Sivanandhan, D. MubarakAli, M. Rajesh, R. Arun, G. Kapildev, M. Manickavasagam, N. Thajuddin, K. Premkumar and A. Ganapathi, *Colloids Surf., B*, 2013, **106**, 86–92.
325 M. Fan, M. Thompson, M. L. Andrade and A. G. Brolo, *Anal. Chem.*, 2010, **82**, 6350–6352.
326 S. Mukherjee, D. Chowdhury, R. Kotcherlakota, S. Patra, B. Vinothkumar, M. P. Bhadra, B. Sreedhar and C. R. Patra, *Theranostics*, 2014, **4**, 316–335.
327 B. Wu, X. Wu, C. Guan, K. F. Tai, E. K. L. Yeow, H. J. Fan, N. Mathews and T. C. Sum, *Nat. Commun.*, 2004, **4**, 1–7.
328 J. Park, M. H. Ullah, S. S. Park and C. Ha, *J. Mater. Sci.: Mater. Electron.*, 2007, **18**, 393–397.
329 K. G. Stamplecoskie and J. C. Scaiano, *J. Phys. Chem. C*, 2011, **115**, 1403–1409.
330 M. Lungu, S. Gavriliu, E. Enescu, M. Lucaci, V. Tsakiris and G. Rimbu, *Metall. Mater. Trans. A*, 2012, 1–6.
331 K. O. Santos, W. C. Elias, A. M. Signori, F. C. Giacomelli, H. Yang and J. B. Domingos, *J. Phys. Chem. C*, 2012, **116**, 4594–4604.
332 A. K. Khan, R. Rashid, G. Murtaza and A. Zahra, *Trop. J. Pharm. Res.*, 2014, **13**, 1169–1177.
333 D. K. Chatterjee, P. Diagaradjane and S. Krishnan, *Ther. Delivery*, 2011, **2**, 1001–1014.
334 E. Ye, M. D. Regulacio, S. Y. Zhang, X. J. Loh and M. Y. Han, *Chem. Soc. Rev.*, 2015, **44**, 6001–6017.
335 M. K. K. Oo, X. Yang, H. Du and H. Wang, *Nanomedicine*, 2008, **3**, 777–786.
336 P. Pandey, S. P. Singh, S. K. Arya, V. Gupta, M. Datta, S. Singh and B. D. Malhotra, *Langmuir*, 2007, **23**, 3333–3337.
337 J. M. Pingarro, P. Y. Seden and A. G. Cortes, *Electrochim. Acta*, 2008, **53**, 5848–5866.
338 Y. Du, L. Shi, M. Hong, H. Li, D. Li and M. Liu, *Opt. Commun.*, 2013, **298–299**, 232–236.
339 W. Cai, T. Gao, H. Hong and J. Sun, *Nanotechnol., Sci. Appl.*, 2008, **1**, 17–32.
340 E. Lima, R. Guerra, V. Lara and A. Guzman, *Chem. Cent. J.*, 2013, **7**, 1–7.
341 C. C. D. Wang, W. C. H. Choy, C. Duan, D. D. S. Fung, W. E. I. Sha, F. X. Xie, F. Huang and Y. Cao, *J. Mater. Chem.*, 2012, **22**, 1206–1211.
342 R. Sharma, V. V. Agrawal, A. K. Srivastava, Govind, L. Nain, M. Imran, S. R. Kabi, R. K. Sinha and B. D. Malhotra, *J. Mater. Chem. B*, 2013, **1**, 464–474.
343 N. Lee and T. Hyeon, *Chem. Soc. Rev.*, 2012, **41**, 2575–2589.
344 D. L. Huber, *Small*, 2015, **1**, 482–501.
345 K. Shrivas, K. Agrawal and H. F. Wu, *Analyst*, 2011, **136**, 2852–2857.
346 T. Lopez, F. Figueras, J. Manjarrez, J. Bustos, M. Alvarez, J. Silvestre Albero, F. Rodriguez Reinoso, A. Martinez Ferre and E. Martinez, *Eur. J. Med. Chem.*, 2010, **45**, 1982–1990.
347 J. C. Claussen, A. Kumar, D. B. Jaroch, M. H. Khawaja, A. B. Hibbard, D. M. Porterfield and T. S. Fisher, *Adv. Funct. Mater.*, 2012, **22**, 3399–3405.
348 S. Mostafa, F. Behafarid, J. R. Croy, L. K. Ono, L. Li, J. C. Yang, A. I. Frenkel and B. R. Cuenya, *J. Am. Chem. Soc.*, 2010, **132**, 15714–15719.
349 K. Q. Peng, X. Wang, X. L. Wu and S. T. Lee, *Nano Lett.*, 2009, **9**, 3704–3709.
350 H. Chen, G. Wei, A. Ispas, S. G. Hickey and A. Eychmuller, *J. Phys. Chem. C*, 2010, **114**, 21976–21981.
351 L. Xu, X. C. Wu and J. J. Zhu, *Nanotechnology*, 2008, **19**, 305603.
352 C. P. Adams, K. A. Walker, S. O. Obare and K. M. Docherty, *PLoS One*, 2014, **9**, e85981.
353 I. F. Ramos, B. C. Montes, M. M. García-Maldonado, C. L. Menendez, A. R. Mayol, L. M. Díaz-Vazquez and C. R. Cabrera, *J. Chem. Educ.*, 2015, **92**, 360–363.
354 S. H. Lim, J. Wei, J. Lin, Q. Li and J. K. You, *Biosens. Bioelectron.*, 2005, **20**, 2341–2346.
355 S. Das, J. M. Dowding, K. E. Klump, J. F. McGinnis, W. Self and S. Seal, *Nanomedicine*, 2013, **8**, 1483–1508.
356 Y. Gao, K. Chen, J. Ma and F. Gao, *OncoTargets Ther.*, 2014, **7**, 835–840.
357 M. S. Wason and J. Zhao, *Am. J. Transl. Res.*, 2013, **5**, 126–131.
358 P. R. Solanki, C. Dhand, A. Kaushik, A. A. Ansari, K. N. Sood and B. D. Malhotra, *Sens. Actuators, B*, 2009, **141**, 551–556.
359 V. Shah, S. Shah, H. Shah, F. J. Rispoli and K. T. McDonnell, *Nanoparticles*, 2012, **7**, 1–13.
360 G. D. Venkatasubbu, S. Ramasamy, V. Ramakrishnan and J. Kum, *Adv. Powder Technol.*, 2013, **24**, 947–954.

361 B. Jana, G. Mondal, A. Biswas, I. Chakraborty and S. Ghosh, *RSC Adv.*, 2013, **3**, 8215–8219.
362 A. Besinis, T. D. Peralta and R. D. Handy, *Nanotoxicology*, 2014, **8**, 1–16.
363 E. Casero, C. Alonso, M. D. Petit-Domínguez, L. Vazquez, A. M. Parra-Alfambra, P. Merino, S. Alvarez-Garcia, A. de Andres, E. Suarez, F. Pariente and E. Lorenzo, *Microchim. Acta*, 2014, **181**, 79–87.
364 M. A. Ibrahem, H. Y. Wei, M. H. Tsai, K. C. Ho, J. J. Shyue and C. W. Chu, *Sol. Energy Mater. Sol. Cells*, 2013, **108**, 156–163.
365 V. Jaskova, L. Hochmannova and J. Vytrasova, *Int. J. Photoenergy*, 2013, **2013**, 795060.
366 X. Ren, D. Chen, X. Meng, F. Tang, X. Hou, D. Han and L. Zhang, *J. Colloid Interface Sci.*, 2009, **334**, 183–187.
367 S. Sahoo, M. Maiti, A. Ganguly, J. J. George and A. K. Bhowmick, *J. Appl. Polym. Sci.*, 2007, **105**, 2407–2415.
368 L. M. Rossi, N. J. S. Costa, F. P. Silva and R. Wojcieszak, *Green Chem.*, 2014, **16**, 2906–2933.
369 A. S. Teja and P. Y. Koh, *Prog. Cryst. Growth Charact. Mater.*, 2009, **55**, 22–45.
370 L. Y. Wang, L. Wang, F. Gao, Z. Y. Yu and Z. M. Wu, *Analyst*, 2002, **127**, 977–980.
371 J. Sun, Y. Zhu, X. Yang and C. Li, *Particuology*, 2009, **7**, 347–352.
372 H. Dhyani, C. Dhand, B. D. Malhotra and P. Sen, *Biosens. Bioelectron.*, 2011, **3**, 1–7.
373 H. Cortinaa, C. M. Alonsoa, M. Castillo-Ortegab and H. Hu, *Mater. Sci. Eng., B*, 2012, **177**, 1491–1496.
374 A. M. Suhail, M. J. Khalifa, N. M. Saeed and O. A. Ibrahim, *Eur. Phys. J.: Appl. Phys.*, 2010, **49**, 1–5.
375 I. Lokteva, N. Radychev, F. Witt, H. Borchert, J. Parisi and J. Kolny-Olesiak, *J. Phys. Chem. C*, 2010, **114**, 12784–12791.
376 M. A. Schreuder, K. Xiao, I. N. Ivanov, S. M. Weiss and S. J. Rosenthal, *Nano Lett.*, 2010, **10**, 573–576.
377 X. J. Loh, T. C. Lee, Q. Dou and G. R. Deen, *Biomater. Sci.*, 2016, DOI: 10.1039/c5bm00277j.
378 J. M. Perez, L. Josephson, T. O'Loughlin, D. Hogemann and R. Weissleder, *Nat. Biotechnol.*, 2002, **20**, 816–820.
379 P. S. Doyle, J. Bibette, A. Bancaud and J. L. Viovy, *Science*, 2002, **295**, 2237.
380 T. J. Yoon, W. Lee, Y. S. Oh and J. K. Lee, *New J. Chem.*, 2003, **27**, 227–229.
381 H. T. Wong, M. K. Tsang, C. F. Chan, K. L. Wong, B. Feic and J. Hao, *Nanoscale*, 2013, **5**, 3465–3473.
382 Q. Q. Dou, C. P. Teng, E. Ye and X. J. Loh, *Int. J. Nanomed.*, 2015, **10**, 419–432.
383 N. M. Idris, M. K. G. Jayakumar, A. Bansal and Y. Zhang, *Chem. Soc. Rev.*, 2015, **44**, 1449–1478.
384 P. Ramasamy, P. Manivasakan and J. Kim, *RSC Adv.*, 2014, **4**, 34873–34895.
385 V. Kumar, G. Toffoli and F. Rizzolio, *ACS Med. Chem. Lett.*, 2013, **4**, 1012–1013.
386 X. Tu, Y. Ma, Y. Cao and J. Huang, *J. Mater. Chem. B*, 2014, **2**, 2184–2192.
387 Q. Dou, X. Fang, S. Jiang, P. L. Chee, T. C. Lee and X. J. Loh, *RSC Adv.*, 2015, **5**, 46817–46822.
388 J. Schuster, G. He, B. Mandlmeier, T. Yim, K. T. Lee, T. Bein and L. F. Nazar, *Angew. Chem., Int. Ed.*, 2012, **51**, 3591–3595.
389 S. K. Bhunia, A. Saha, A. R. Maity, S. C. Ray and N. R. Jana, *Sci. Rep.*, 2012, **3**, 1–7.
390 X. Zhao, L. Yang, X. Li, X. Jia, L. Liu, J. Zeng, J. Guo and P. Liu, *Bioconjugate Chem.*, 2015, **26**, 128–136.
391 M. Das, C. Dhand, N. Dwivedi, B. P. Singh, G. Sumana, V. V. Agarwal, J. S. Tawale and B. D. Malhotra, *Sens. Actuators, B*, 2015, **210**, 281–289.
392 C. I. C. Crucho, *ChemMedChem*, 2015, **10**, 24–38.
393 C. Dhand, M. P. Prabhakaran, R. W. Beuerman, R. Lakshminarayanan, N. Dwivedi and S. Ramakrishna, *RSC Adv.*, 2014, **4**, 32673–32689.
394 M. Elsabahy and K. L. Wooley, *Chem. Soc. Rev.*, 2012, **41**, 2545–2561.
395 K. Wang, X. Zhang, X. Zhang, B. Yang, Z. Li, Q. Zhang, Z. Huang and Y. Wei, *J. Mater. Chem. C*, 2015, **3**, 1854–1860.
396 K. Lia and B. Liu, *Chem. Soc. Rev.*, 2014, **43**, 6570–6597.